The discrimination of chromatic textures

Martin Giesel Department of Psychology, Justus-Liebig-University, Giessen, Germany

Thorsten Hansen Department of Psychology, Justus-Liebig-University, Giessen, Germany

Karl R. Gegenfurtner Department of Psychology, Justus-Liebig-University, Giessen, Germany

Color discrimination is influenced by chromatic distributions such as they appear on differently illuminated 3D surfaces (T. Hansen, M. Giesel, & K. R. Gegenfurtner, 2008). Here, we measured discrimination thresholds for chromatically variegated stimuli and modeled the data employing a model with multiple chromatic mechanisms. Each mechanism has a differently tuned half-wave-rectified cosine-shaped sensitivity profile centered at a different chromatic direction. To estimate thresholds, the model's responses to a test and a comparison stimulus are determined. A detection variable is calculated by taking the difference of the responses to the two stimuli and by a subsequent nonlinear combination of the responses. The model was fitted to the data presented in T. Hansen et al. (2008) and to data from two new experiments. In the first experiment, we measured discrimination thresholds for stimuli chromatically variegated along a direction orthogonal to the one used in the previous experiments. In the second experiment, we investigated the interplay between chromatic distributions and different mean contrast levels. We found that a model with eight mechanisms accounted for the effect of chromatic variation within the stimuli and provided a better fit to the discrimination thresholds than a four mechanisms model.

Keywords: chromatic discrimination, chromatic distributions, discrimination model, higher level mechanisms, tuning width

Citation: Giesel, M., Hansen, T., & Gegenfurtner, K. R. (2009). The discrimination of chromatic textures. *Journal of Vision,* 9(9):11, 1–28, http://journalofvision.org/9/9/11/, doi:10.1167/9.9.11.

Introduction

The most fundamental laws of color vision are Grassmann's laws of color matching (Grassmann, 1853). A consequence of Grassmann's laws is that any light can be represented as a vector in a three-dimensional space that is spanned by three primary lights (Wandell, 1982). Various attempts to model chromatic discrimination of small chromatic differences are based on the line element approach that makes use of the vectorial representation of colors. The basic idea of the line element theory is that the length of the difference vector between the vectors that represent two colors provides a measure of the perceived difference between these colors. However, in this basic form, line element models predict identical thresholds independent of the location in color space where discrimination thresholds are measured. Since this is not in accordance with discrimination data that show that thresholds increase with increasing intensity of the stimuli as predicted by Weber's law, line element models were modified to incorporate a transformation of the vector differences to account for the state of adaptation of the visual mechanisms that are thought to mediate chromatic discrimination.

Early examples of line element models were based on the output of the photoreceptors (Helmholtz, 1896; Schrödinger, 1920; Stiles, 1946). Later work suggests that not the photoreceptors but the responses of second stage cone-opponent color mechanisms determine discrimination thresholds (Boynton & Kambe, 1980; LeGrand, 1968; MacLeod & Boynton, 1979; Noorlander & Koenderink, 1983). Models that are based on the output of the second stage chromatic mechanisms are, e.g., the models by Guth, Massof, and Benzschawel (1980), Jameson and Hurvich (1955), Koenderink, van de Grind, and Bouman (1972), and Vos and Walraven (1972a, 1972b).

The second stage cone-opponent mechanisms are sometimes referred to as the "cardinal directions of color space" (Krauskopf, Williams, & Heeley, 1982). These directions correspond to independent mechanisms whose neural substrate is postulated to originate in the cone-opponent cells in the retina and the lateral geniculate nucleus (Derrington, Krauskopf, & Lennie, 1984). Originally, the cardinal mechanisms were conceived of as three bipolar mechanisms (two chromatic and one achromatic) lying along the cardinal directions of color space. However, the studies by Krauskopf (1980), Krauskopf et al. (1982), and Sankeralli and Mullen (2001) provided evidence for separate unipolar mechanisms along the half-axes of the cardinal directions, resulting in four chromatic mechanisms in the isoluminant plane. In the following, we refer to these unipolar directions when we talk about cardinal mechanisms. In modeling approaches, unipolar

doi: 10.1167/9.9.11 Received February 12, 2009; published August 24, 2009 ISSN 1534-7362

mechanisms are generally modeled using half-wave rectification.

Derrington et al. (1984) showed that the majority of LGN cells sum their inputs in a linear fashion. Results from numerous psychophysical experiments using different methods provided evidence for the existence of mechanisms in addition to the cardinal mechanisms (e.g., D'Zmura, 1991; D'Zmura & Knoblauch, 1998; Gegenfurtner & Kiper, 1992; Goda & Fujii, 2001; Hansen & Gegenfurtner, 2005, 2006; Krauskopf & Gegenfurtner, 1992; Krauskopf, Williams, Mandler, & Brown, 1986; Krauskopf, Wu, & Farell, 1996; Krauskopf, Zaidi, & Mandler, 1986; Li & Lennie, 1997; Lindsey & Brown, 2004; Mizokami, Paras, & Webster, 2004; Monaci, Menegaz, Süsstrunk, & Knoblauch, 2004; Webster & Mollon, 1991, 1994; Zaidi & Halevy, 1993; Zaidi & Shapiro, 1993). This is in accordance with results from electrophysiological experiments (Gegenfurtner, Kiper, & Levitt, 1997; Kiper, Fenstemaker, & Gegenfurtner, 1997; Komatsu, 1998; Komatsu, Ideura, Kaji, & Yamane, 1992; Lennie, Krauskopf, & Sclar, 1990; Wachtler, Sejnowski, & Albright, 2003), which show that the chromatic preferences of cortical neurons in various cortical areas vary over a wide range whereas the chromatic preferences of retinal ganglion cells and LGN cells cluster around the two cardinal directions of color space (Derrington et al., 1984).

The responses of most V1 cells (Johnson, Hawken, & Shapley, 2001, 2004; Lennie et al., 1990) and most V2 cells (Kiper et al., 1997) to chromatic modulations are well accounted for by a model postulating a linear combination of the signals derived from the three cone classes. Although there are some V1 cells that are more selective for color than predicted (Cottaris & De Valois, 1998), a linear model adequately fits the responses of the majority of V1 cells. In V2, two thirds of the cells have a bandwidth close to that predicted by the linear model, the bandwidth of the other third is significantly narrower (Kiper et al., 1997). For these cells, an extended model that includes a nonlinear stage is necessary to fit the data.

Here, we measured discrimination thresholds at various locations in color space to determine the number and properties of the mechanisms that mediate chromatic discrimination. Krauskopf and Gegenfurtner (1992) measured chromatic discrimination under controlled adaptation conditions at the adaptation point and at various test locations away from the adaptation point. At test locations with chromatic directions intermediate to the cardinal axes, discrimination ellipses were elongated in the test direction. This suggests that discrimination is mediated by more than the four cardinal mechanisms. Moreover, they found differences between different intermediate test locations. For test locations on a diagonal lying exactly intermediate to the cardinal axes and along which colors vary between magenta and greenish (first diagonal), discrimination ellipses were more rounded whereas on the orthogonal diagonal along which colors vary between bluish and yellowish (second diagonal), discrimination ellipses were more elongated.

In most previous studies, both the measurement and the modeling of chromatic discrimination was based on homogeneously colored stimuli. However, only few objects in our environment are homogeneously colored. Instead, they exhibit a distribution of chromaticities and luminances due to changes in illumination or material (Kingdom, 2008). There are only a few studies using chromatically variegated stimuli to investigate chromatic discrimination (Hansen, Giesel, & Gegenfurtner, 2008; Li & Lennie, 1997; tePas & Koenderink, 2004; Zaidi & Shapiro, 1993; Zaidi, Spehar, & DeBonet, 1998). In Hansen et al. (2008), discrimination thresholds were measured for uniformly colored disks and stimuli with a distribution of chromaticities. These stimuli were either photographs of natural objects or synthetic chromatic textures. The chromaticities of these stimuli varied along the second diagonal in the isoluminant plane of the DKL color space (135°–315°). This choice was motivated by the finding that the chromaticities of most fruit and vegetable images had their main chromatic variation approximately along this direction.

One aim of these experiments was to determine whether there is a difference between discrimination thresholds for well-known natural objects and synthetic stimuli with chromatic distributions similar to those of the natural stimuli. Differences in color appearance between natural objects and synthetic stimuli have been reported for achromatic settings by Hansen, Olkkonen, Walter, and Gegenfurtner (2006), but for chromatic discrimination we found no differences in thresholds for natural and synthetic objects. For both synthetic and natural stimuli with a distribution of chromaticities centered at the adaptation point, discrimination ellipses exhibited an elongation in the direction of the chromatic distribution compared with the almost circular discrimination ellipse for the homogeneously colored disk. Away from the adaptation point, the discrimination ellipses for all stimuli were similarly elongated in the direction of the shift away from the adaptation point, but as found by Krauskopf and Gegenfurtner (1992) there was an asymmetry between discrimination ellipses at test locations on the first and second diagonal. These results indicate that the putative intermediate mechanisms have different properties.

Previously, we also tested chromatic distributions with different directions at the adaptation point. Although we found an elongation in the direction of the chromatic distribution for all distributions, discrimination ellipses for different directions differed in shape and size. The most prominent difference was between the ellipses for stimuli chromatically variegated along the first and the second diagonal, respectively. Discrimination ellipses for chromatic variation along the first diagonal were less elongated than ellipses for chromatic variation along the second diagonal. Here, we complement the previous results by measuring chromatic discrimination thresholds

away from the adaptation point for stimuli chromatically variegated along the first diagonal to see whether this distribution also causes differences in thresholds away from the adaptation point compared with thresholds for stimuli chromatically variegated along the second diagonal.

The previous experiments showed a change in the direction in which the discrimination ellipses were elongated depending on whether the test location was at the adaptation point or away from it. In the second experiment, we investigated at which pedestal contrast this change in direction occurs and how it is influenced by the amplitude of the chromatic distribution by measuring discrimination thresholds for chromatic distributions with different amplitudes at various pedestal contrasts.

The results presented here indicate that chromatic distributions can affect chromatic discrimination thresholds in a considerable way. Models of chromatic discrimination should account for the effects of chromatic distributions to make them feasible to a wider range of applications. Here, we present an approach to modeling thresholds for small color differences. The input to the model are the signals from the second stage cone-opponent mechanisms. We show that this model provides a good fit to the discrimination data for both homogeneously colored and chromatically variegated stimuli presented in Hansen et al. (2008) and to data from the two new experiments. We found that a model with eight mechanisms fitted the data better than a model with only the four cardinal mechanisms.

Methods

Experiment 1

Apparatus

The software for stimulus presentation was programmed in Matlab using the Psychophysics toolbox extensions (Brainard, 1997, Pelli, 1997). The stimuli were displayed on a SONY GDM-F520 color CRT monitor. The monitor resolution was set to 1024 × 768 pixels with a refresh rate of 75 Hz noninterlaced. The monitor was controlled by a PC using a Cambridge Research Bits++ graphics card providing a 14-bit resolution for each color channel. The monitor was calibrated using a Cambridge Research OptiCal photometer. For each of the three primaries, the spectra were measured at their maximum intensity with a Photo Research PR 650 spectroradiometer. The obtained spectra were then multiplied with the Judd-revised CIE 1931 color matching functions (Judd, 1951; Wyszecki & Stiles, 1982) to derive CIE *xyY* coordinates of the monitor phosphors. The *xyY* coordinates of the monitor primaries at maximum intensity are given by R = (0.6164, 0.3492, 19.35), G = (0.2829, 0.606, 48.309), and B = (0.155, 0.0796, 7.0614). The *xyY* coordinates were then used to convert between RGB and DKL color space.

Color space

All stimuli were described in the isoluminant plane of the DKL color space (Derrington et al., 1984; Krauskopf et al., 1982). The DKL color space is a second stage cone-opponent color space, which reflects the preferences of retinal ganglion cells and LGN neurons. It is spanned by an achromatic luminance axis, the L + M axis, and two chromatic axes, the L − M axis and the S − (L + M) axis. The two chromatic axes define an isoluminant plane. These three axes that represent the cardinal directions of color space as defined by Krauskopf et al. (1982) intersect at the white point. The L + M axis is determined by the sum of the signals generated by the long wavelength cones (L-cones) and the middle wavelength cones (M-cones). The L − M axis is determined by the differences in the signals generated by the L-cones and the M-cones. Along the L − M axis, the L- and M-cone excitations covary at a constant sum, while the S-cone excitation does not change. Colors along the L − M axis vary between reddish and bluish-greenish. The S − (L + M) axis is determined by the differences in the signals generated by the short wavelength cones (S-cones) and the sum of the L- and M-cones. Along the S − (L + M) axis, only the excitation of the S-cones changes and colors vary between yellow-greenish and purple. Within the isoluminant plane colors are commonly defined by polar coordinates of azimuth and amplitude. The azimuth defines the chromatic direction and can be related to hue changes. The azimuth or chromatic direction is 0° for positive excursions along the L − M axis and ranges in a counterclockwise direction from 0° to 360°. The amplitude is given by the distance from the white point at the origin and can be related to changes in saturation. Here, the axes of the DKL color space were arbitrarily scaled from −1 to 1, where ±1 corresponds to the maximum contrast achievable on the monitor used. The relationship between these coordinates and the device-independent coordinates (r, b) as suggested by MacLeod and Boynton (1979) are depicted in the top part of Figure 1, with sample data showing average detection thresholds at the white point for four observers for a uniformly colored disk. Since the data presented here are related to the data presented in Hansen et al. (2008) and the setups used in the two studies differed, we also show in the bottom part of Figure 1 the detections thresholds measured in the previous study. The thresholds were essentially identical.

Stimuli

The stimuli were isoluminant circular patches either uniformly colored or chromatically variegated along the chromatic direction 45°–225° (variation along the first diagonal) and 135°–315° (variation along the second diagonal), respectively. The amplitude of the chromatic distribution was 0.25. The variegated stimuli had a $1/f^2$ amplitude spectrum (brown noise). This amplitude spectrum

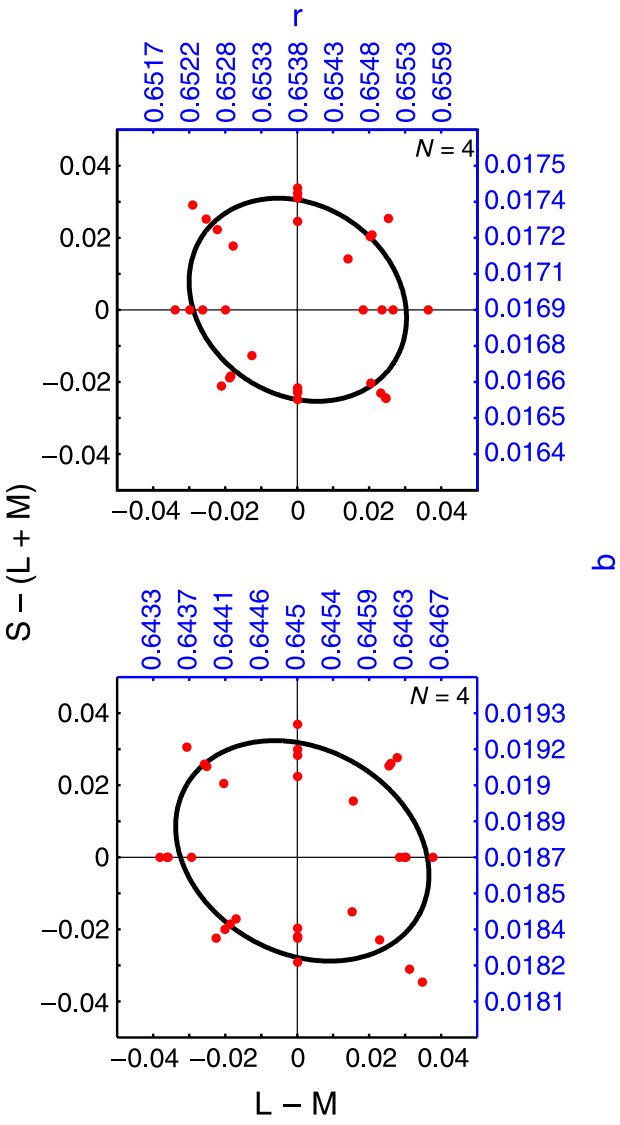

Figure 1. Detection thresholds at the adaptation point for eight comparison directions (top). The stimulus was a uniformly colored disk. The ellipse was fitted to the pooled thresholds of four observers (C.H., D.P., D.P.E., M.G.). The figure on the bottom shows the same detection thresholds for the disk measured in Hansen et al. (2008) using a different setup (bottom). The ellipse was fitted to the pooled thresholds of four observers (C.H., D.P., M.G., M.O).

was chosen because in the previous experiments we found the largest effect of the chromatic distribution on thresholds for stimuli with an amplitude spectrum of $1/f^2$. The chromatic textures were generated by adjusting the particular noise texture distribution to the desired chromatic distribution. First, we generated an achromatic noisy texture with a white noise distribution. For $1/f^2$ noise, this distribution was then Fourier transformed, the amplitude spectrum was reweighted for each frequency to the desired slope, and the result was transformed back to the spatial domain using the inverse Fourier transformation. The stimuli had a size of 153 × 153 pixels and subtended 3.5° of visual angle. The edges of the stimuli were blurred with a Gaussian low-pass filter with standard deviation of 3 pixels. A new version of the noise image was generated in each trial. This rules out that thresholds were influenced by the recurrence of the patterns.

Figure 2 shows examples of the two types of chromatically variegated stimuli, their chromatic histograms, and chromatic distributions in the isoluminant plane of the DKL color space. Note, that the L − M and S − (L + M) histograms for stimuli with an amplitude spectrum similar to $1/f^2$ vary between different realizations of the stimuli.

Observers

Three observers (C.H., D.P.E., and M.G.) participated in the first experiment. All but one (M.G.) were naïve as to the purpose of the experiment. Not all experiments were done by all observers. All observers had normal or corrected-to-normal vision and normal color vision as tested with Ishihara plates.

Procedure

The procedure was similar to the one employed by Hansen et al. (2008) and Krauskopf and Gegenfurtner (1992). Observers were seated in front of the monitor at a distance of 1 m in a dark room and instructed to fixate the fixation point at the center of the screen, which was uniformly gray colored. The monitor was placed in a viewing tube. The inside of the tube was painted in black and the front of the tube was covered by black cloth. The observers viewed the monitor through an opening in the cloth. In each experimental trial, four stimuli were presented for 500 ms in a 2 × 2 arrangement on top of a homogeneous gray background of 37 cd/m^2. The eccentricity of the centers of the stimuli was 4.5° of visual angle. Three of the presented stimuli were identical (test stimuli) while the fourth one (comparison stimulus) differed slightly in chromaticity. The position of the comparison stimulus in the 2 × 2 arrangement was randomly varied in each trial. For the chromatically variegated stimuli, the four stimuli presented in the 2 × 2 arrangement were mirrored in such a way that corresponding pixels of the textures had the same distance from the fixation point at each location. The observer's task was to indicate the position of the comparison stimulus (odd one out) by pressing the appropriate one of four buttons. Visual feedback was given after each response. Test and comparison chromaticities were specified in the isoluminant plane of the DKL color space. The chromaticities of the comparison stimulus were varied by a rigid shift of the whole chromatic distribution in the isoluminant plane in the direction of the particular comparison color. This transformation shifts the mean of the distribution to the comparison color but preserves the position of the chromaticities relative to the mean chromaticity. We measured thresholds for eight comparison

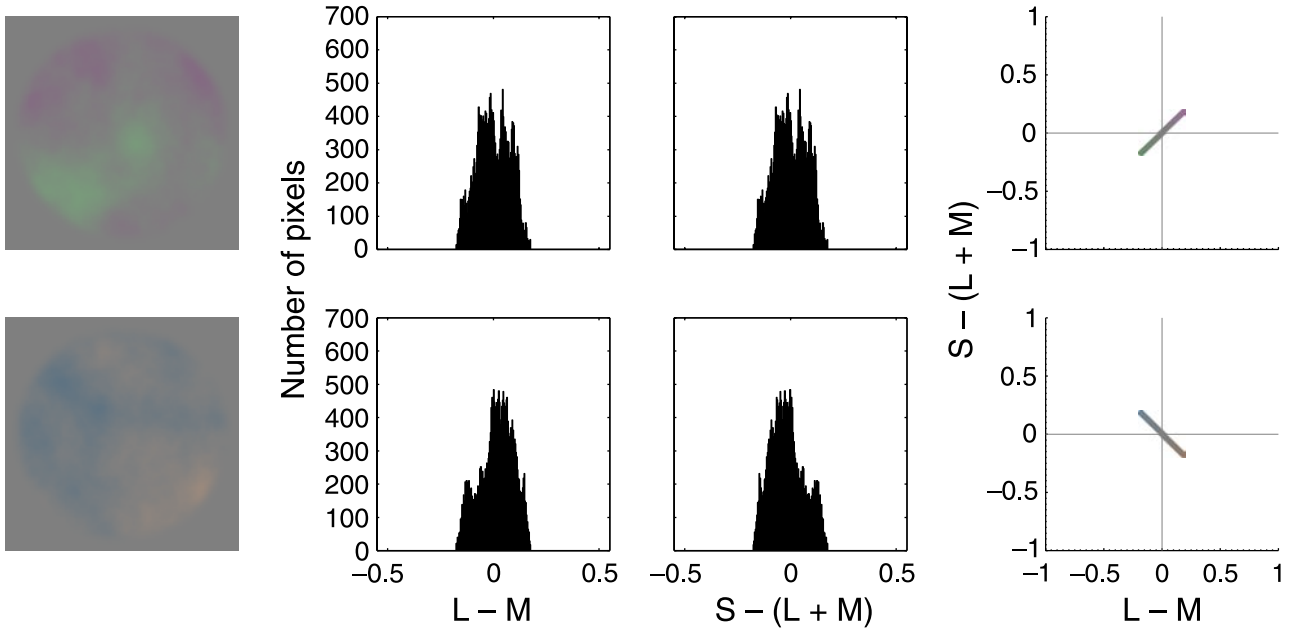

Figure 2. Examples of the $1/f^2$ noise stimuli (first column), L − M histograms (second column), S − (L + M) histograms (third column), and chromatic distributions in the isoluminant plane of the DKL color space (fourth column). The chromatic variation of the stimuli was along the first diagonal (45°–225°; first row) or along the second diagonal (135°–315°) (second row). The amplitude of the chromatic distribution was 0.25 for both types of stimuli. A new version of the noise distribution was generated in each trial. Note that the chromaticities of the stimuli varied only along a line in color space. There was no additional variation in other directions. The contrast of the images has been enhanced for better visibility.

directions (0°, 45°, 90°, 135°, 180°, 225°, 270°, and 315°). The amount or amplitude of this shift necessary for a correct discrimination at 79% of the trials was determined using an adaptive double-random staircase procedure (Levitt, 1971). After three consecutive correct responses, the comparison amplitude was decreased by 0.1 log units; after an incorrect response, it was increased by 0.1 log units. In each session, one up and one down staircase for each of the eight comparison directions were randomly interleaved. Each staircase terminated after seven reversals.

Discrimination thresholds were measured under two conditions of adaptation. In the first condition, chromatic discrimination was measured at the adaptation point; in the second condition, discrimination was measured at test locations away from the adaptation point. In the first condition, discrimination was investigated at the location in color space to which the observer was adapted, i.e., the test color was the same as the color of the background (test amplitude of zero), and the comparison stimuli were excursions from the chromaticity of the background. For the homogeneously colored disk, this condition corresponds to a detection task. For the chromatically variegated stimuli, the mean chromaticity of the stimuli was the same as the chromaticity of the background. In the second regime, the test stimuli were excursions from the adaptation point into different test directions. In this condition, the mean chromaticity of all stimuli differed from the chromaticity of the adaptation point. The chromatic directions of these test locations were 0°, 45°, 90°, 135°, 180°, 225°, 270°, and 315°, respectively. The test amplitude was 0.5 for all test directions.

Data analysis

To determine thresholds, the observers' responses for the up and the down staircase were pooled for each comparison direction. Psychometric functions were fitted to the individual observer's data using the psignifit toolbox for Matlab (Wichmann & Hill, 2001) to derive 79% difference thresholds for each of the comparison directions. To summarize the data, ellipses were fitted to the eight thresholds using a direct least-squares procedure (Halíř & Flusser, 1998). As in previous studies (Knoblauch & Maloney, 1996; Poirson, Wandell, Varner, & Brainard, 1990), we found that the ellipses describe the data well. To account for small asymmetries, the centers of the ellipses were allowed to vary. To obtain ellipses for data averaged across observers, ellipses were fitted to the pooled thresholds of all observers, as suggested by some authors as being the most robust method (Wyszecki & Fielder, 1971; Wyszecki & Stiles, 1982; Xu, Yaguchi, & Shioiri, 2002).

Experiment 2

The same setup was used in the second experiment as in the first experiment.

Stimuli

Figure 3 shows examples of the two types of chromatically variegated stimuli, their chromatic histograms, and chromatic distributions in the isoluminant plane of the DKL color space.

The stimuli were either homogeneously colored disks or stimuli whose chromaticities varied along the second diagonal. The amplitude of the chromatic distribution was either 0.25 or 0.5. The stimuli were generated in the same way as in the first experiment but the amplitude spectrum of the variegated stimuli was similar to a 1/*f* spectrum (pink noise). The L − M and S − (L + M) histograms of stimuli with an amplitude spectrum similar to 1/*f* can be approximated by a normal distribution. We normalized the noise histograms of the two types of variegated stimuli so that each type had the same standard deviation in each trial, respectively. A further reason for using 1/*f* noise is that it has been found that images of natural scenes have a characteristic amplitude spectrum that falls off with approximately 1/*f* (Field, 1989; Ruderman & Bialek, 1994; Tolhurst, Tadmor, & Chao, 1992). All other spatial and temporal aspects of the stimuli were identical to those in Experiment 1.

Observers

Seven observers (C.H., D.K., D.P., M.G., M.O., N.L., and S.B.) participated in the experiments. All but one (M.G.) were naive as to the purpose of the experiment. Not all experiments were done by all observers. All observers had normal or corrected-to-normal vision. Color vision was tested by using the Ishihara plates.

Procedure

For two observers (D.P. and M.G.), discrimination thresholds were measured at the adaptation point and at test locations away from the adaptation point for two test directions (0° and 315°), five test amplitudes (0, 0.05, 0.1, 0.25, and 0.5), and eight comparison directions (0°, 45°, 90°, 135°, 180°, 225°, 270°, and 315°). For seven observers (C.H., D.K., D.P., M.G., M.O., N.L., and S.B.), discrimination thresholds were measured at the adaptation point and at test locations away from the adaptation point for test direction 315° at 10 test amplitudes (0, 0.05, 0.10, 0.15, 0.20, 0.25, 0.30, 0.35, 0.40, and 0.50) but only for increment and decrement comparison directions (315° and 135°), i.e., the direction of the shift away from the adaptation point and the direction of the chromatic distribution of the stimuli were collinear. The comparison directions were randomly interleaved within an experiment. The same adaptive staircase procedure as in the first experiment was used. A staircase terminated after six reversals.

At a test amplitude of 0.5, some pixels of the comparison stimuli for the 1/*f* noise stimulus whose

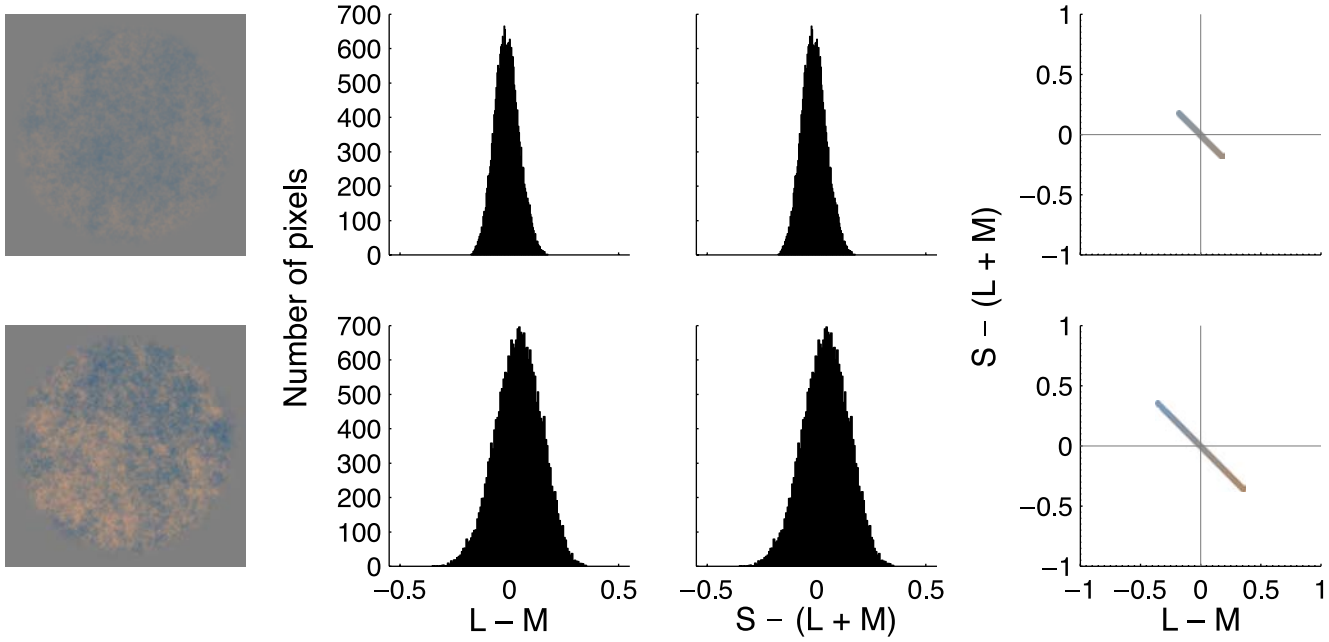

Figure 3. Examples of the 1/*f* noise stimuli with chromatic variation along the second diagonal (135°–315°) (first column), L − M histograms (second column), S − (L + M) histograms (third column), and chromatic distributions in the isoluminant plane of the DKL color space (fourth column). The chromatic amplitude was either 0.25 (first row) or 0.5 (second row). Note that the chromaticities of the stimuli varied only along a line in color space. A new version of the noise distribution was generated in each trial. The contrast of the images has been enhanced for better visibility.

chromatic distribution had an amplitude of 0.5 exceeded the gamut of the monitor for some comparison amplitudes. These pixels were mapped to the nearest reproducible chromaticity. Since the chromatic histogram of the 1/*f* noise stimuli is close to a normal distribution, this affected only a small proportion of the pixels. For test direction 0° and comparison direction 0°, the distance to which the comparison stimulus could be shifted away from the test location without exceeding the gamut was smallest (approximately 0.2). Since for all test and comparison directions the observers' thresholds were several steps of the staircase below the values at which the overflow occurred, we accepted this shortcoming to be able to test sufficiently different stimuli at a wide range of test locations.

Since our stimuli were presented to the parafovea, it could be argued that the use of the Judd-revised CIE 1931 color matching functions, which were optimized for foveal vision, might not represent the optimal choice of color matching functions and might have resulted in an isoluminant plane that was tilted with respect to isoluminance so that differences in luminance could have contributed to the discriminability.

We compared the Judd-revised color matching functions with the CIE 1964 10° color matching functions by computing the CIELAB differences between our stimuli using both the Judd-revised color matching functions and the CIE 1964 color matching functions for the conversion to CIELAB. The luminance contrasts between these stimuli are relatively small, but they may be at or above threshold. However, for the task in our experiments the luminance differences between the test stimuli and the comparison stimuli at each test location are of importance. The stimuli defined by the CIE 1964 primaries will lie on a plane in our original Judd-based color space. This plane is tilted with respect to the nominal isoluminant plane. For the stimuli we use, this tilt results in potential luminance differences of 1–3 cd/m^2. However, both the test and the comparison stimuli would lie within that same plane, and therefore their differences are indeed much smaller than that, typically around 0.1 cd/m^2. This is way beyond anything that could be useful for these comparisons.

Model

The first goal of this paper is to describe a model that accounts for the effect of chromatic distributions on discrimination thresholds. In the following, we outline a model with multiple chromatic mechanisms and show that it provides a good fit to the data presented in Hansen et al. (2008). The model belongs to the group of geometric or vector models of chromatic discrimination (Graham, 1989; Wandell, 1982). It is derived from the chromatic detection models presented in D'Zmura and Knoblauch (1998), Goda and Fujii (2001), and Hansen and Gegenfurtner (2006) and is close to the one presented by Chen, Foley, and Brainard (2000a, 2000b).

Description of the model

The core components of the model are multiple chromatic mechanisms that are sensitive to second-order cone-opponent features as represented by the isoluminant plane of the DKL color space. The model assumes M mechanisms that are defined in the isoluminant plane of the DKL color space. Each mechanism i has a half-wave-rectified cosine shaped sensitivity profile S_i centered around the peak sensitivity μ_i. The sensitivity S_i of mechanism i centered at μ_i to the chromatic direction θ is given by

$$S_i(\theta) = s_i[\cos^{k_i}(\theta - \mu_i)]^+. \quad (1)$$

The centers of the mechanisms were equally spaced in the isoluminant plane of the DKL color space. We tested model variants with four and eight mechanisms. For $M = 4$, the centers were at $\mu_i = 0°$, 90°, 180°, and 270° and for $M = 8$ at $\mu_i = 0°$, 45°, 90°, 135°, 180°, 225°, 270°, and 315°. The parameter k_i determines the tuning width of the sensitivity profile (D'Zmura & Knoblauch, 1998) for mechanism i. If k is equal to one, the sensitivity function has a half-width at half-height (HWHH) of 60°. Larger values of k describe more narrowly tuned functions. The sensitivity parameter s multiplicatively scales the area under the sensitivity function for each mechanism individually.

To determine the excitation of each mechanism, the images were converted to DKL chromaticities. The chromaticities of each pixel were described by its chromatic direction in the isoluminant plane (azimuth) and the chromatic amplitude (saturation) of the vector originating at the white point. The excitation E_i of mechanism i was computed by multiplication of the chromatic amplitude r of each pixel j of the stimulus with the sensitivity S_i of this mechanism to the chromatic direction θ of the pixel. The excitations were summed across the pixels of the stimulus for each mechanism separately. The resulting excitation of the mechanism was divided by the number of pixels of the stimulus to provide an average response to the image that is independent of the image size. The excitatory response E_i of mechanism i to the image was given by

$$E_i = \frac{1}{N}\left(\sum_{j=1}^{N} r_j S_i(\theta_j)\right), \quad (2)$$

where N is the number of pixels, r_j is the chromatic amplitude and θ_j is the chromatic direction of the jth pixel.

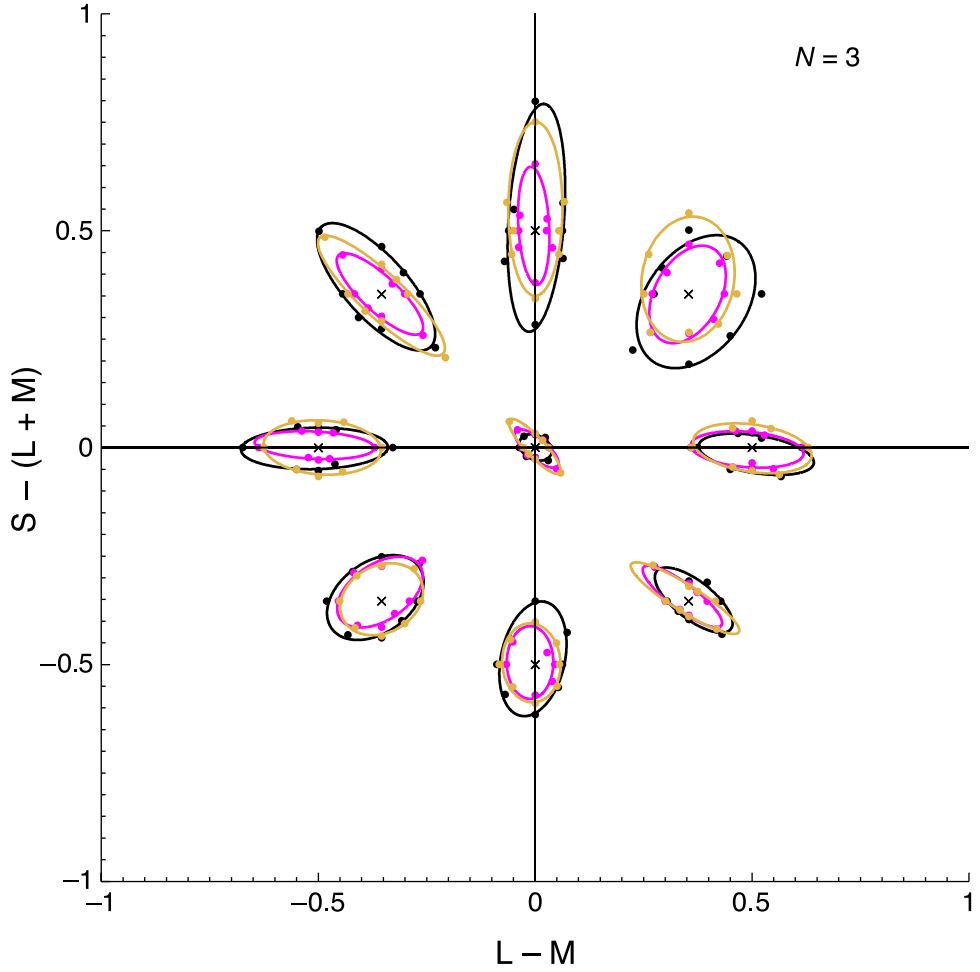

Figure 4. Discrimination ellipses at the adaptation point and at eight test locations away from the adaptation point for an uniformly colored disk (black), $1/f$ (pink), and $1/f^2$ (yellow) noise textures. The crosses indicate the chromaticity at the test location. Data points are discrimination thresholds averaged across three observers (C.H., M.G., M.O.). The curve is the best fit ellipse to the thresholds.

We used a power response function as proposed by Legge (1981) for luminance contrast discrimination to compute the responses of the mechanisms

$$R_i = gE_i^p. \tag{3}$$

The parameters g, p were the same for all mechanisms.

Assuming a 2AFC task, responses were computed in this way both for the test stimulus and the comparison stimulus. The use of 2AFC in the model instead of the 4AFC task that was used in the experiments presented here and in Hansen et al. (2008) is justified because the three test stimuli were identical except for the mirroring. Since the model computes the mean responses of the mechanisms to an image and does not account for differences in retinal eccentricity or in the spatial configuration of the stimuli, it would respond in the same way to the three test stimuli. Thus, computing the difference in excitation between the comparison stimulus and each of the three test stimuli would be redundant.

To compute the detection variable D, the responses to the test stimulus (R_{T_i}) and the comparison stimulus (R_{C_i}) were subtracted for each mechanism separately. The individual mechanisms' responses were combined using a Minkowski metric with an exponent of $Q = 2$ (Euclidean distance). Threshold was defined as the lowest contrast where the detection variable D was equal to one

$$D = \left(\sum_{i=1}^{M} |R_{C_i} - R_{T_i}|^2 \right)^{\frac{1}{2}}. \tag{4}$$

Data

We simultaneously fitted the model to the discrimination data for the disk and to the chromatically variegated stimuli with the $1/f$ and $1/f^2$ amplitude spectrum presented in Hansen et al. (2008). The data were averaged across the three observers for the different types of stimuli. In Hansen et al., discrimination was also measured for the

image of a banana. The results for this stimulus were comparable to the results for the chromatically variegated stimuli. Therefore, we excluded the data for the banana from the fit. Figure 4 shows the discrimination ellipses for the three types of stimuli averaged across the observers. Altogether, the model was fitted to 216 data points using the Matlab function lsqnonlin.

The images that were used as input to the model were generated in the same way as described in the Method section. The images were either of one uniform color or were chromatically variegated along the second diagonal (135°–315°) with an amplitude of 0.25. The chromatically variegated stimuli had an amplitude spectrum similar to either $1/f$ or $1/f^2$. The size of the input images used in the fitting procedure was 25 × 25 pixels. We reduced the size of the input images compared with the size of the stimuli used in the experiment for faster computation. Since the responses of the mechanisms are averaged across the pixels, the size of the images should not affect the fit. We have compared fits for images of different sizes and found no significant effects of the image size.

Model predictions

The fitted parameters for the two model variants are shown in Table 1. The tuning width parameter k is given as half-width at half-height (HWHH) with HWHH = 60° for $k = 1$. With the exception of the mechanism at 90°, for both model variants the cardinal mechanisms were more narrowly tuned than expected by a linear combination of cone inputs. In addition, the model with eight mechanisms had narrowly tuned mechanisms along the second diagonal and broadly tuned mechanisms along the first diagonal. The values of the sensitivity parameter s reflected the higher sensitivity of the mechanisms in the lower two quadrants (225°, 270°, and 315°).

Figure 5 shows the discrimination ellipses predicted by a model with four mechanisms and by a model with eight mechanisms for the disk and stimuli with chromatic variation along the second diagonal. Although the discrimination data for the stimuli with an amplitude spectrum similar to $1/f$ were included in the data set to which the model was fitted, we do not present the results for this stimulus type here. Since our model does not contain a spatial frequency transformation, the predicted discrimination ellipses for $1/f$ noise stimuli were identical to the ellipses predicted for the corresponding $1/f^2$ noise stimuli which are shown here.

In contrast to the eight mechanisms model, the four mechanisms model did not predict the narrow ellipse at the adaptation point for the stimuli with chromatic variation along the second diagonal and the elongated ellipses on the second diagonal at test locations 135° and 315° for both types of stimuli.

To evaluate the goodness of the fit, we computed the bias corrected version of Akaike's information criterion (AIC_c) (Akaike, 1974; Burnham & Anderson, 2002, 2004), which penalizes a model for additional parameters, for the models with four and eight mechanisms using

$$AIC_c = n\log\left(\frac{RSS}{n}\right) + 2K + \frac{2K(K+1)}{n-K-1}, \quad (5)$$

where $n = 216$ is the number of data points in the data set, K is the number of parameters that were fitted, and RSS is the residual sum of squares. Additionally, we also computed the Bayesian information criterion (BIC) using

$$BIC = n\log\left(\frac{RSS}{n}\right) + K\log(n). \quad (6)$$

The results are shown in Table 2.

The lower AIC_c and BIC values for the model with eight mechanisms indicate that this model provided a better fit to the data compared with the model with four mechanisms despite the larger number of parameters.

	$M = 4$	$M = 8$
Response function		
g	24.795	20.139
p	0.578	0.599
Tuning width (HWHH)		
k_0	50.795	34.367
k_{45}	–	52.032
k_{90}	59.325	73.036
k_{135}	–	28.924
k_{180}	48.263	34.298
k_{225}	–	61.165
k_{270}	49.372	48.679
k_{315}	–	30.947
Sensitivity		
s_0	21.524	11.777
s_{45}	–	24.982
s_{90}	15.914	5.324
s_{135}	–	14.083
s_{180}	20.876	8.782
s_{225}	–	21.841
s_{270}	31.068	30.530
s_{315}	–	18.733

Table 1. Parameters for the model with four and the model with eight mechanisms. g and p are the parameters of the response function, k_i is the tuning width of the sensitivity function given as half-width at half-height (HWHH), and s_i is the sensitivity of the ith mechanism.

Discussion

We modeled the discrimination data for homogeneous stimuli and chromatically variegated stimuli using a model with multiple chromatic mechanisms. The inputs

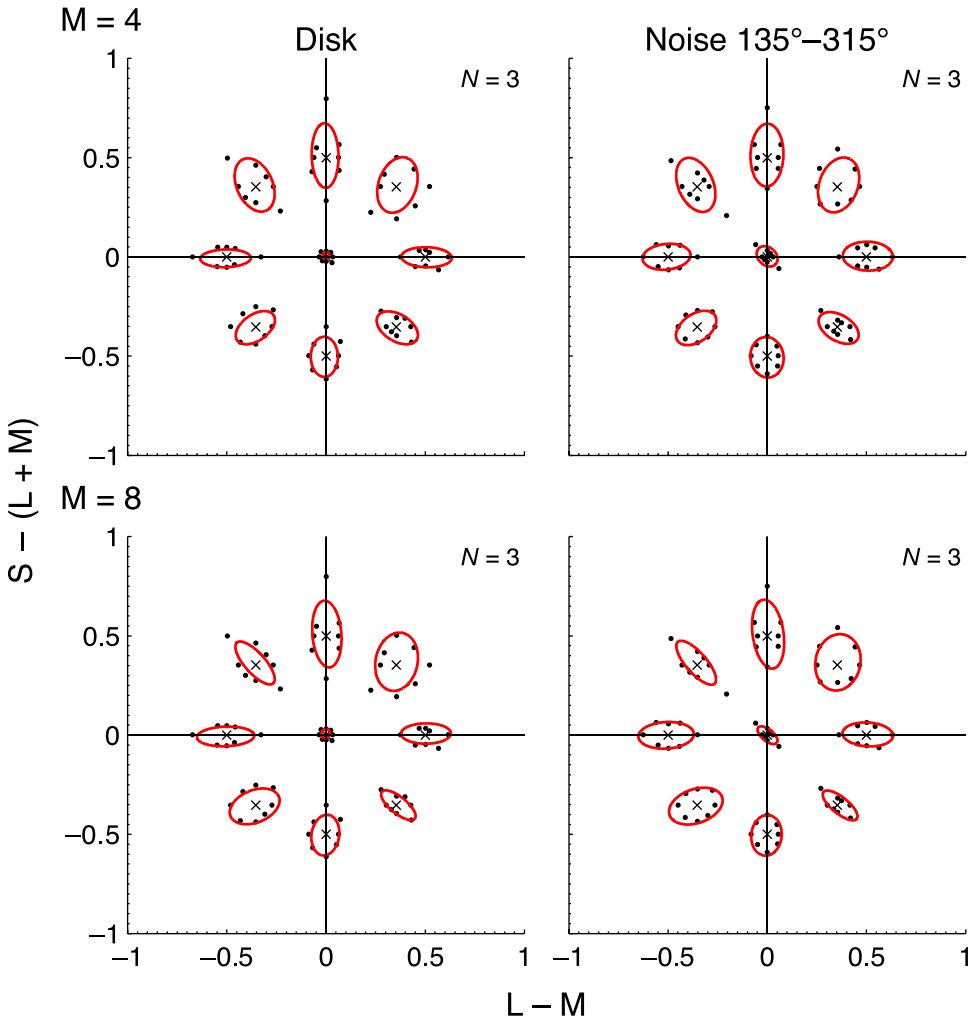

Figure 5. Discrimination thresholds (black dots) at the adaptation point and away from the adaptation point for the disk (first column) and for stimuli with chromatic variation along the second diagonal (second column) averaged across three observers. Discrimination ellipses show discrimination contours (red ellipses) fitted to the thresholds predicted by a model with four mechanisms (first row) and by a model with eight mechanisms (second row). Crosses indicate the test location.

to the model were the responses of the second-order cone-opponent mechanisms as represented by the DKL color space. We were interested in showing that a model based on vector differences between the excitations of chromatic mechanisms can describe discrimination thresholds for chromatically variegated stimuli and in determining whether the discrimination data for uniform and chromatically variegated stimuli could be modeled using a model with only the four cardinal mechanisms or whether it is necessary to assume higher level mechanisms along intermediate directions. The model was fitted to the data presented in Hansen et al. (2008).

M	RSS	*K*	AIC_c	BIC	ΔAIC_c	ΔBIC
8	15.933	18	−523.61	−466.33	0	0
4	25.397	10	−441.31	−408.63	82.31	57.70

Table 2. Evaluation of the model variants using Akaike's information criterion (AIC_c) and the Bayesian information criterion (BIC). *M* gives the number of mechanisms in the model, RSS is the residual sum of squares, *K* is the number of parameters in the model, and AIC_c and BIC are the information criteria as defined by Equations 5 and 6, respectively. ΔAIC_c and ΔBIC were computed as the difference between AIC_c and min(AIC_c) and between BIC and min(BIC), respectively.

Quantitatively, the lower AIC_c and BIC values for the model with eight mechanisms indicated that this model outperformed the four mechanisms model despite the larger number of parameters. Qualitatively, the results show that the model with four mechanisms neither predicted the narrowly elongated ellipse for the chromatically variegated stimuli at the adaptation point nor the differently tuned discrimination ellipses at test locations on the first and second diagonal. In the four mechanisms model, the discrimination ellipses on the first and second

diagonal were similar in the upper two and lower two quadrants, respectively.

The number of eight mechanisms is at best a lower bound for the actual number of mechanisms. We also fitted a model with 16 mechanisms. This did not improve the fit, which is not surprising since we only measured at eight test locations with chromatic directions similar to the centers of the mechanisms. This allows no predictions about discrimination performance at test locations intermediate to these eight directions.

The parameters g and p of the response function account for the increase in thresholds with increasing distance from the adaptation point. These parameters were only slightly different for the two model variants. There was a tendency toward more narrowly tuned cardinal mechanisms in the eight mechanisms model. This was most obvious for mechanisms at 0° and 180°.

In addition, the model with eight mechanisms had broadly tuned mechanisms on the first diagonal (45°–225°), which corresponds to the almost circular discrimination ellipses at test locations 45° and 225°. The mechanisms on the second diagonal (135°–315°) were narrowly tuned in accordance to the narrow discrimination ellipses at test locations 135° and 315°. The smaller discrimination ellipses in the lower two quadrants are reflected by the higher sensitivity parameters of the mechanisms in these quadrants. For both model variants, there was an asymmetry between the tuning widths and sensitivities of the mechanisms at 90° and 270°. While for both the four and the eight mechanisms model, the mechanisms at 0° and 180° had similar tuning widths and sensitivity values, the mechanisms at 90° and 270° differed considerably in both parameters with the mechanism at 90° having a broader tuning and reduced sensitivity compared with the mechanism at 270°. However, the discrimination performance at a specific test location cannot be simply deduced from the properties of the mechanism at this location but also depends on the properties of the mechanisms which are activated concurrently.

Kiper et al. (1997) showed that the chromatic preferences of neurons in V2 and V3 span the full color circle. There are no distinct chromatic directions around which these preferences cluster as they do in the LGN (Derrington et al., 1984), rather there is a continuum of preferences. Therefore, the confinement of the mechanisms in our model to equally spaced chromatic directions is to some degree arbitrary and simplistic. One might think of the centers of the mechanisms as mean chromatic directions of different subsets of neurons. The model could be easily extended to incorporate the varying chromatic preferences of neurons by allowing the centers of the mechanisms to vary. The model has further shortcomings in that it accounts neither for the retinal eccentricity of the stimuli nor for their spatial characteristics. We are planning to integrate these aspects in future versions of the model.

Experiment 1

In the previous experiments (Hansen et al., 2008), the chromatic variation of the stimuli tested away from the adaptation point was along the second diagonal (135°–315°). Away from the adaptation point, we found no systematic differences in size or orientation of the discrimination ellipses between stimuli chromatically variegated along the second diagonal and the homogeneously colored disk. Here, we measured discrimination for stimuli chromatically variegated along the first diagonal (45°–225°), i.e., orthogonal to the direction of the chromatic distribution previously used. The choice of a chromatic distribution variegated along the first diagonal was motivated by the finding that the discrimination ellipse for this stimulus at the adaptation point was different from the ellipse for the stimulus with chromatic variation along the second diagonal in that the ellipse was less elongated (Hansen et al., 2008). This might be indicative of differences in discrimination ellipses away from the adaptation point. Moreover, the use of chromatic distributions that are orthogonal to each other provides a clue to the number of mechanisms that mediate discrimination because the two distributions produce the same excitation of the cardinal mechanisms at intermediate test locations. Therefore, any differences in the discrimination ellipses for the two types of stimuli at these test locations suggest the existence of mechanisms at intermediate directions.

Results

Figure 6 shows the results for discrimination at the adaptation point separately for three observers. The stimuli were homogeneously colored disks, stimuli chromatically variegated along the first diagonal, and stimuli chromatically variegated along the second diagonal (see Figure 2).

The discrimination ellipses for the disk were almost circular for all three observers, indicating similar discrimination thresholds for the eight comparison directions. The discrimination ellipses for the chromatically variegated stimuli were elongated. This elongation was approximately into the direction of the chromatic distribution of the stimuli. The discrimination ellipses for chromatic variation along the second diagonal were more elongated than the ellipses for stimuli varying along the first diagonal. While the thresholds for the comparison directions orthogonal to the chromatic distribution for the stimuli with the chromatic distribution along the second diagonal were close to the thresholds for the disk, the discrimination thresholds for these directions for stimuli varying along the first diagonal were more elevated.

Figure 7 shows the discrimination thresholds for stimuli with chromatic variation along the first diagonal at eight test locations away from the adaptation point, separately

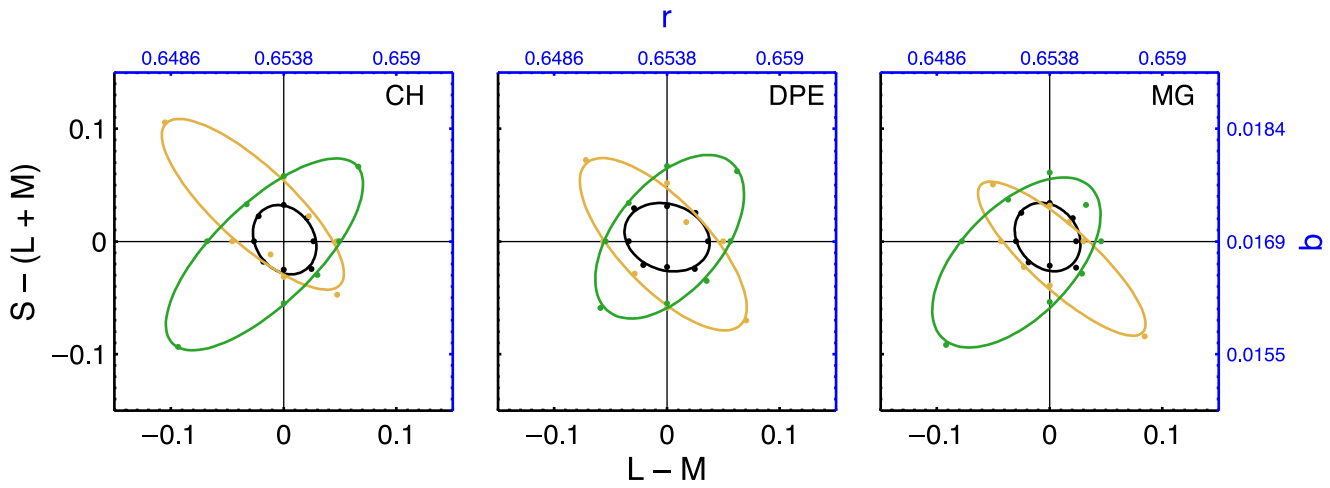

Figure 6. Discrimination thresholds at the adaptation point for three observers. The stimuli were homogeneously colored disks (black), stimuli chromatically variegated along the first diagonal (green), and stimuli chromatically variegated along the second diagonal (yellow). The filled symbols indicate the thresholds for the eight comparison directions.

for three observers. These results complement the results presented in Hansen et al. (2008; see Figure 4). For comparison, we show the discrimination ellipses at the adaptation point already shown in Figure 6, again. For observer D.P.E., we also measured discrimination ellipses away from the adaptation point for the disk and stimuli with chromatic variation along the second diagonal. The results for observers C.H. and M.G. for these stimuli are shown in Figure 4.

Thresholds away from the adaptation point were elevated compared with the thresholds at the adaptation point. While stimuli at the adaptation point showed an elongation in the direction of the chromatic distribution, discrimination ellipses away from the adaption point were in general elongated in the direction of the contrast axis connecting the test location to the origin. However, at some test locations (90°, 180°), the ellipses exhibited a slight tilt into the direction of the chromatic distribution. In accordance to previous findings, thresholds in the upper two quadrants were higher than in the lower two quadrants. For the stimuli with chromatic variation along the first diagonal, the discrimination ellipses at test locations 45° and 225°, i.e., the direction of the chromatic variation of the stimuli, were more elongated than the ellipses at test locations 135° and 315°.

The results for observer D.P.E. show that at all test locations away from the adaptation point the discrimination ellipses for chromatic variation along the first

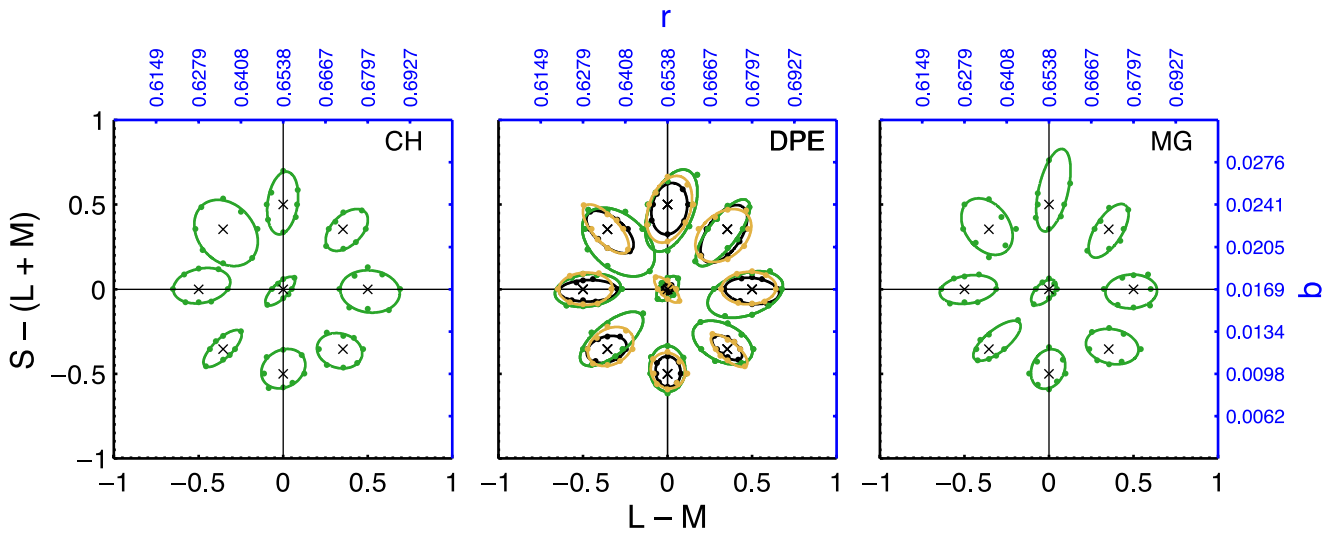

Figure 7. Discrimination thresholds at the adaptation point and at eight test locations away from the adaptation point for the stimulus with chromatic variation along the second diagonal (green) separately for three observers. The filled symbols show the thresholds for the eight comparison directions. The crosses indicate the chromaticity at the test location. Additionally, for observer D.P.E. discrimination ellipses for the disk (black) and stimuli with chromatic variation along the second diagonal (yellow) are shown.

diagonal were larger than the ellipses for the disk and stimuli with chromatic variation along the second diagonal. The elevation in thresholds is most clearly visible for test directions orthogonal to the first diagonal (135° and 315°). These differences can be more clearly seen in Figure 8 where the area and eccentricity of the ellipses is plotted against the location of the test colors. Area and eccentricity were computed from ellipses fitted to the individual observers discrimination data and than averaged across observers (C.H., D.P.E., M.G.). The data for the disk and stimuli chromatically variegated along the second diagonal for observers C.H. and M.G. were collected with a different setup (see Figure 4). The areas of the ellipses for the disk and stimuli chromatically variegated along the second diagonal were similar at test locations away from the adaptation point. The area of the ellipses was smaller in the lower two quadrants than in the upper two quadrants. For stimuli chromatically variegated along the first diagonal, the area was elevated compared with the other stimuli at most test locations away from the adaptation point. The plot of the eccentricity of the ellipses against the test locations shows a differential effect of the two types of chromatically variegated stimuli away from the adaptation point. The ellipses for the chromatically variegated stimuli were more elongated when the chromatic variation was collinear to the test direction (i.e., test directions 45° and 225° for stimuli variegated along the first diagonal and test directions 135° and 315° for stimuli variegated along the second diagonal) and less elongated when the chromatic variation was orthogonal to the test direction (i.e., test directions 135° and 315° for stimuli variegated along the first diagonal and test directions 45° and 225° for stimuli variegated along the second diagonal). This indicates that there was an effect of the chromatic distributions away from the adaptation point which points to the existence of mechanisms tuned to intermediate directions. The ellipses for stimuli varying along the second diagonal were, at most test locations away from the adaptation point, similar to the ellipses for the disk both in area and eccentricity. In contrast, the ellipses for stimuli chromatically variegated along the first diagonal were considerably elevated compared with the other stimuli. This speaks for a lower sensitivity to chromatic variation along the first diagonal.

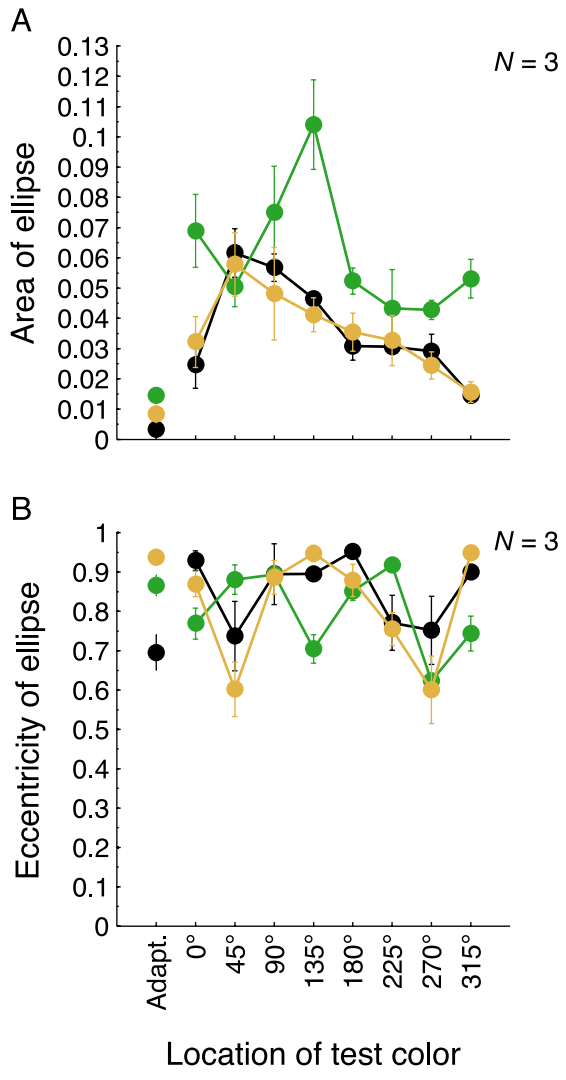

Figure 8. Area (A) and eccentricity (B) of the discrimination ellipses for the disk (black), stimuli chromatically variegated along the first diagonal (green), and stimuli chromatically variegated along the second diagonal (yellow) averaged across three observers (C.H., D.P.E., M.G.). Note that the discrimination ellipses for the disk and stimuli chromatically variegated along the second diagonal for observers C.H. and M.G. were collected using a different setup (see Figure 4). Error bars denote standard error of the mean.

Discussion

The results show that discrimination thresholds were lowest at the adaptation point and increased at test locations away from the adaptation point. There is a systematic difference between discrimination thresholds for homogeneously colored stimuli and chromatically variegated stimuli at the adaptation point in that discrimination ellipses for the latter were elongated in the direction of the chromatic distribution. These findings corroborate the results presented in Hansen et al. (2008).

The important feature of the new results is that we found effects of the chromatic distributions at test locations away from the adaptation point. In Hansen et al. (2008), we found no evidence for that. In the previous study, all chromatically variegated stimuli that were tested away from the adaptation point varied mainly along the second diagonal. At test locations away from the adaptation point the discrimination ellipses for these stimuli were similar to the ellipses for the disk. The same pattern of results was found for these stimuli in the present experiment for observer D.P.E. Here, we complemented the previous results by measuring discrimination thresholds for stimuli

with a chromatic distribution orthogonal to the one previously employed. Thresholds for chromatic variation along the first diagonal were elevated compared with thresholds for the disk and the thresholds for chromatic variation along the second diagonal at most test locations. This is most obvious for test locations on the second diagonal. These findings indicate that sensitivity to chromatic variation along the first diagonal is decreased compared with sensitivity to chromatic variation along the second diagonal. The differences in the area of the discrimination ellipses at different test locations indicate that the mechanisms also differ in their sensitivities. Particularly noticeable is that for all types of stimuli, thresholds in the lower two quadrants were lower than in the upper two quadrants.

The results substantiate the notion of the existence of higher level chromatic mechanisms tuned to chromatic directions intermediate to the cardinal axes because we found ellipses clearly elongated along intermediate directions. If there were only mechanisms tuned to the cardinal directions of color space, either discrimination ellipses should be circular or the maximal elongation of the discrimination ellipses should be preferentially in the direction of the cardinal mechanisms. Moreover, the ellipses at intermediate directions varied in area and eccentricity depending on the direction of the chromatic distribution of the stimuli. This also indicates that there are mechanisms tuned to intermediate directions since the cardinal mechanisms do not respond differentially to the two chromatic distributions.

Experiment 2

Both the results of Experiment 1 and of Hansen et al. (2008) show differences in the orientations of discrimination ellipses for chromatically variegated stimuli at the adaptation point and at test locations away from the adaptation point in that discrimination ellipses at the adaptation point were elongated in the direction of the chromatic distribution whereas ellipses away from the adaptation point were elongated in the direction of the contrast axis. We hypothesize that discrimination thresholds for chromatically variegated stimuli were determined by two noise components. One of the components can be attributed to the chromatic variation within the stimuli and the other one can be attributed to the increase in thresholds with increasing distance from the adaptation point as predicted by Weber's law. The first component caused the elongation of the discrimination ellipses in the direction of the chromatic distribution at the adaptation point, and the second component caused the elongation of the ellipses in the direction of the contrast axis.

In the second experiment, we set out to disentangle the interplay between the properties of chromatic distributions and the contrast of the test stimuli by measuring threshold versus contrast (TvC) functions for chromatically variegated stimuli with different amplitudes of the chromatic distribution (see Figure 3) and homogeneously colored stimuli at various pedestal contrasts.

Results

Figure 9 shows the results for test direction 0° for the three types of stimuli for two observers. For simplicity, in the following we refer to the 1/*f* noise stimuli with the lower chromatic amplitude of the chromatic distribution as pink noise 0.25 and to the 1/*f* noise stimuli with the higher amplitude as pink noise 0.5.

The discrimination ellipses were smallest at the adaptation point and increased in size with increasing distance from the adaptation point for all stimuli. At the adaptation point, the discrimination ellipse for the disk was almost circular whereas the ellipses for the chromatically variegated stimuli were elongated in the direction of the chromatic distribution. This elongation was larger for the stimulus with the higher chromatic amplitude. With increasing distance from the adaptation point, the discrimination ellipses for the disk became more elongated in the direction of the shift away from the adaptation point. With increasing test amplitude, the ellipses for the chromatically variegated stimuli rotated away from an elongation in the direction of the chromatic distribution toward an elongation in the test direction. The test amplitude where the ellipse for pink noise 0.25 is no longer elongated in the direction of the chromatic distribution but elongated in the test direction was between test amplitude 0.1 and 0.25. For pink noise 0.5, the ellipse at the highest test amplitude still showed a slight tilt into the direction of the chromatic distribution. Due to gamut limitations, we could not measure discrimination at higher test amplitudes.

Figure 10 shows the thresholds presented in Figure 9 separately for each of the eight comparison directions averaged across the two observers.

The increase in thresholds was largest for comparison directions collinear to the test direction (comparison directions 0° and 180°). Beginning from a certain test amplitude, for the chromatically variegated stimuli, these thresholds outweighed the initially larger thresholds for comparison directions collinear to the direction of the chromatic distribution (comparison directions 135° and 315°) resulting in a tilt of the discrimination ellipse toward the test direction. The results show a difference in the TvC functions for increment and decrement directions. For decrement directions where the shift in the comparison direction produced a stimulus that was closer to the adaptation point than the test stimulus (comparison directions 180°, 135°, and 225°), thresholds increased in a linear fashion. For increment test directions where the shift in the comparison direction produced a stimulus

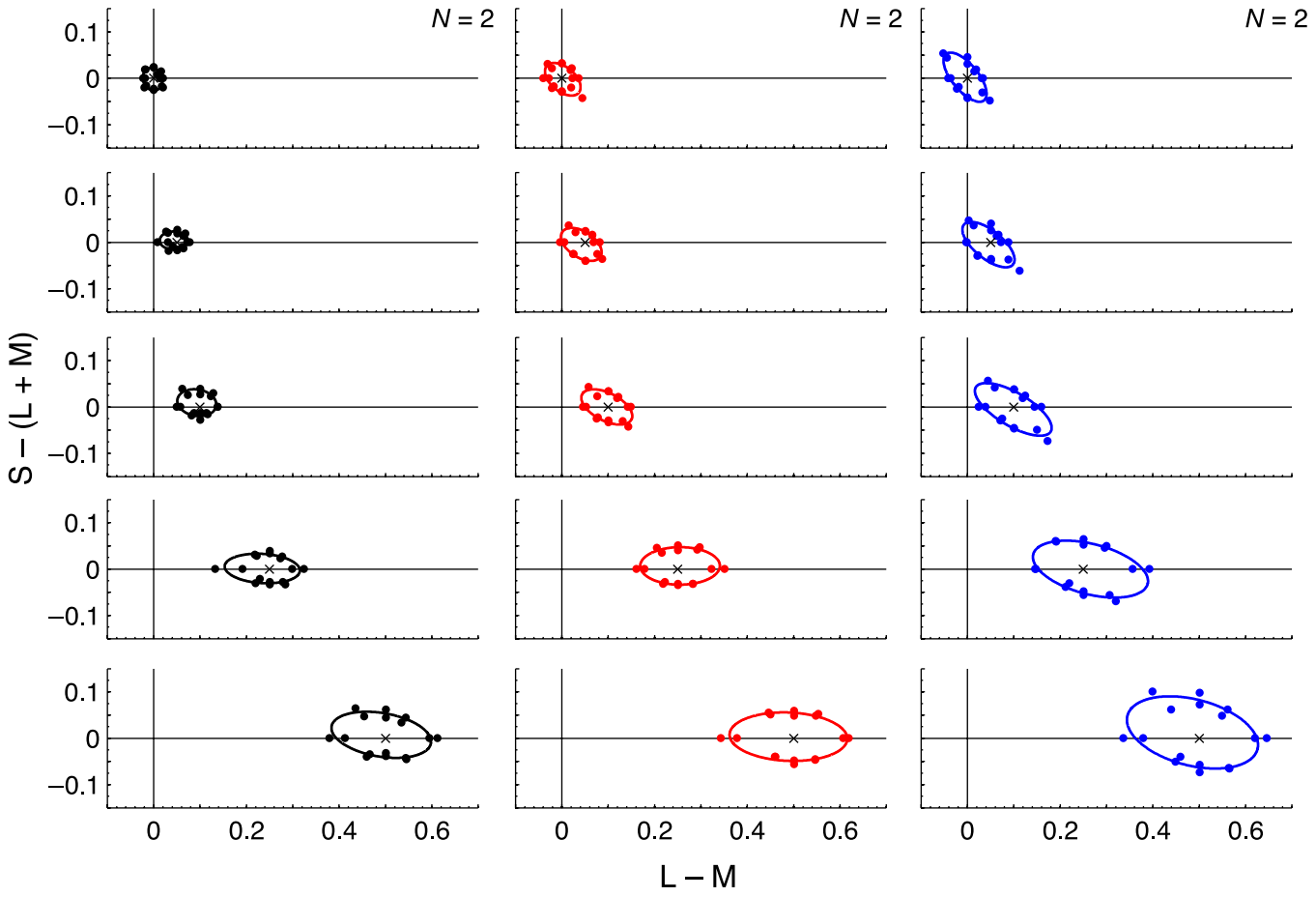

Figure 9. Discrimination ellipses for test direction 0° at the adaptation point (first row) and at different test amplitudes away from the adaptation point (rows from top to bottom: 0, 0.05, 0.1, 0.25, and 0.5) for the disk (black), pink noise 0.25 (red), and pink noise 0.5 (blue). Ellipses were fitted to the pooled thresholds of two observers (D.P. and M.G.). Filled symbols indicate the individual observers' thresholds for the eight comparison directions. The crosses mark the chromaticity at the test location. For the chromatically variegated stimuli, this was the mean chromaticity of their chromatic distribution.

further away from the adaptation point than the test stimulus, the TvC functions saturated for higher test amplitudes.

Figure 11 shows the results for test direction 315° for the three types of stimuli for two observers.

Since in this condition the chromatic distribution is collinear to the test direction, thresholds for comparison directions 135° and 315° increased almost exclusively. At the adaptation point, the discrimination ellipse for the disk is circular, and the ellipses for the variegated stimuli were elongated in the direction of the chromatic distribution. With increasing distance from the adaption point, thresholds for comparison directions 135° and 315° increased for all stimuli.

Figure 12 shows the thresholds presented in Figure 11 separately for each of the eight comparison directions averaged across the two observers.

Except for comparison directions 135° and 315°, thresholds for the three types of stimuli were almost identical and scarcely affected by the increase in test amplitude. For the decrement direction 135°, thresholds increased in a linear manner except for the peak at test amplitude 0.05 for the disk. For the increment direction 315°, thresholds for the disk increased linearly besides the dipper at test amplitude 0.05. The thresholds for the chromatically variegated stimuli saturated at higher test amplitudes.

We measured thresholds for test direction 315° in more detail at 10 test amplitudes but only for the increment and decrement comparison directions 315° and 135°. Figure 13 shows the increment and decrement thresholds for the three types of stimuli averaged across seven observers.

The pattern of the results was similar to the TvC functions shown in Figure 12 showing the dipper at test location 0.05 and a saturating TvC function for comparison direction 315° and a nearly linear increase in thresholds for comparison direction 135°. Statistical analysis using the Friedman test showed a significant difference on the 5% level between the three types of stimuli across all test amplitudes. Multiple comparisons revealed that this difference is mainly due to the difference between the thresholds for the disk and pink noise 0.5.

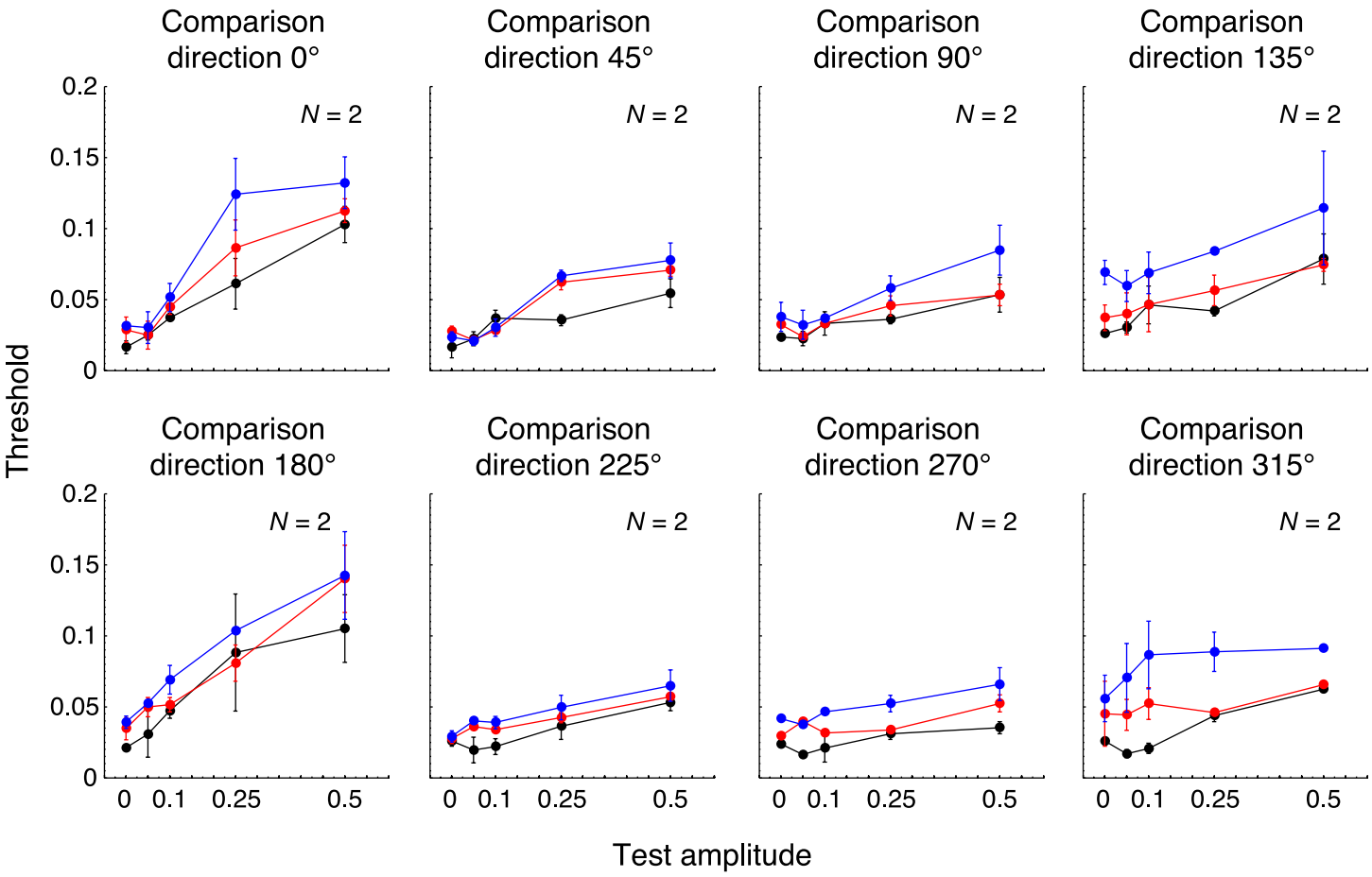

Figure 10. Discrimination thresholds for test direction 0° separately for each of eight comparison directions at the adaptation point (test amplitude of zero) and at test locations away from the adaptation point for the disk (black), pink noise 0.25 (red), and pink noise 0.5 (blue). Filled symbols indicate thresholds for the particular test location averaged across two observers (D.P. and M.G.). Error bars show the standard error of the mean. Note that the direction of the chromatic variation of the pink noise stimuli was along the second diagonal corresponding to comparison directions 135° and 315° (fourth column).

Thresholds for pink noise 0.25 were neither significantly different from thresholds for the disk nor from thresholds for pink noise 0.5.

Discussion

We measured discrimination ellipses at various test locations away from the adaptation point for a homogeneously colored disk and two types of chromatically variegated stimuli that differed in the amplitude of their chromatic distribution. At the adaptation point, thresholds were highest in the direction of the chromatic distribution whereas at test locations away from the adaptation point these thresholds were dominated by an elevation of thresholds in the direction of the shift away from the adaptation point (see Figures 9 and 10). The test location at which thresholds in the direction of the shift away from the adaptation point outweighed the effect of the chromatic distribution depended on the amplitude of the chromatic distribution. This point was reached at a lower test amplitude for the 1/*f* noise stimulus with the lower chromatic amplitude of the distribution than for the stimulus with the higher chromatic amplitude. For the stimulus with the higher chromatic amplitude, the ellipse at test location 0.5 still showed an effect of the chromatic distribution. As noted above, at this test location, results for this stimulus type might have been influenced by the mapping of pixels that were out of gamut.

Thresholds in the direction of the shift away from the adaptation point increased with increasing test amplitude. This effect is shown by the increasing elongation of the discrimination ellipses for the disk in Figures 9 and 11. Figures 10, 12, and 13 show that this increase was approximately linear for the disk.

The peak at test amplitude 0.05 for the decrement test direction 135° might be an artifact. At this test amplitude for some comparison amplitudes, the comparison stimulus is indistinguishable from the background, which might have led observers to make a comparison only between the three test stimuli and thus might have caused the

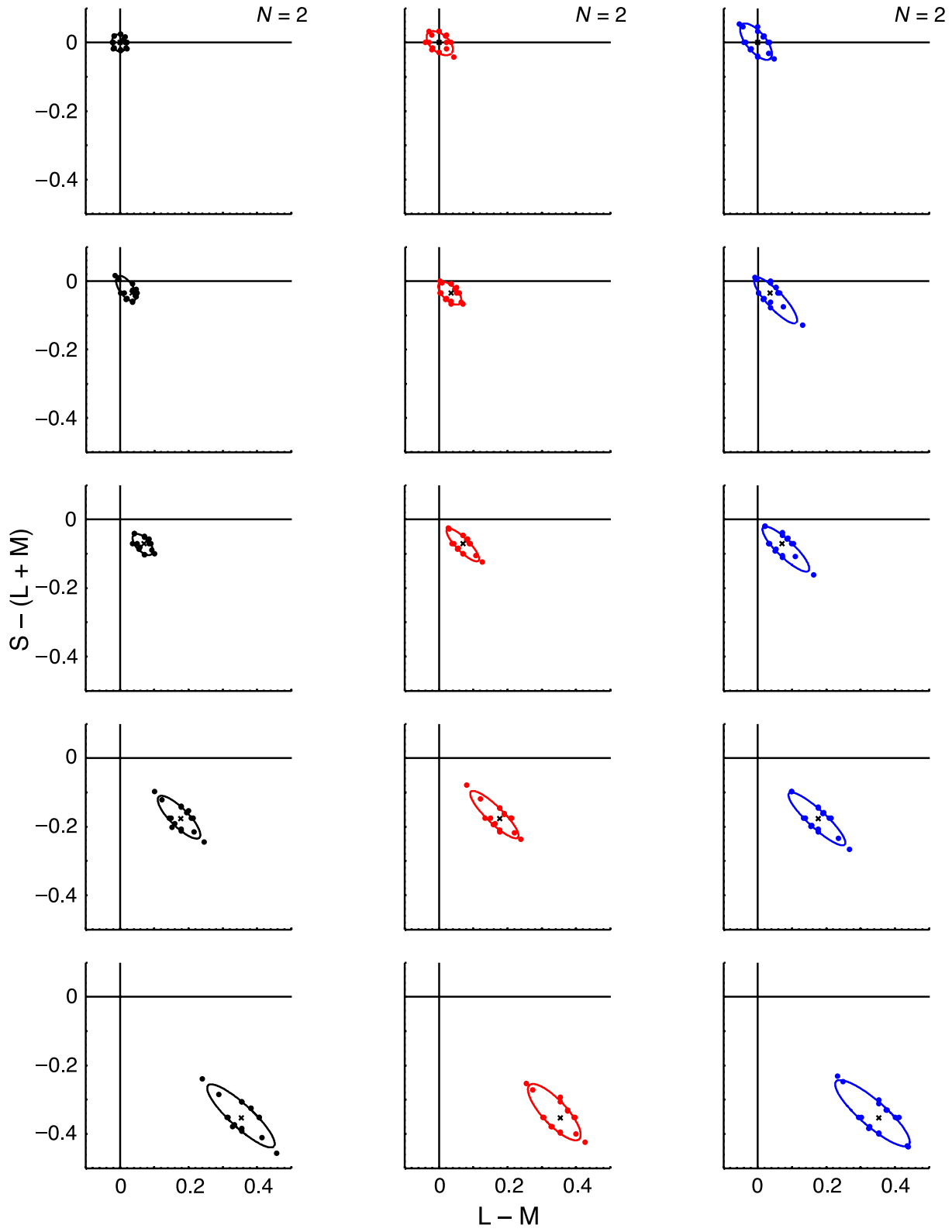

Figure 11. Discrimination ellipses for test direction 315° at the adaptation point (first row) and at different test amplitudes away from the adaptation point (rows from top to bottom: 0, 0.05, 0.1, 0.25, and 0.5) for the disk (black), pink noise 0.25 (red), and pink noise 0.5 (blue). Ellipses were fitted to the pooled thresholds of two observers (D.P. and M.G.). Filled symbols indicate the individual observers' thresholds for the eight comparison directions. The crosses mark the chromaticity at the test location. For the chromatically variegated stimuli, this was the mean chromaticity of their chromatic distribution.

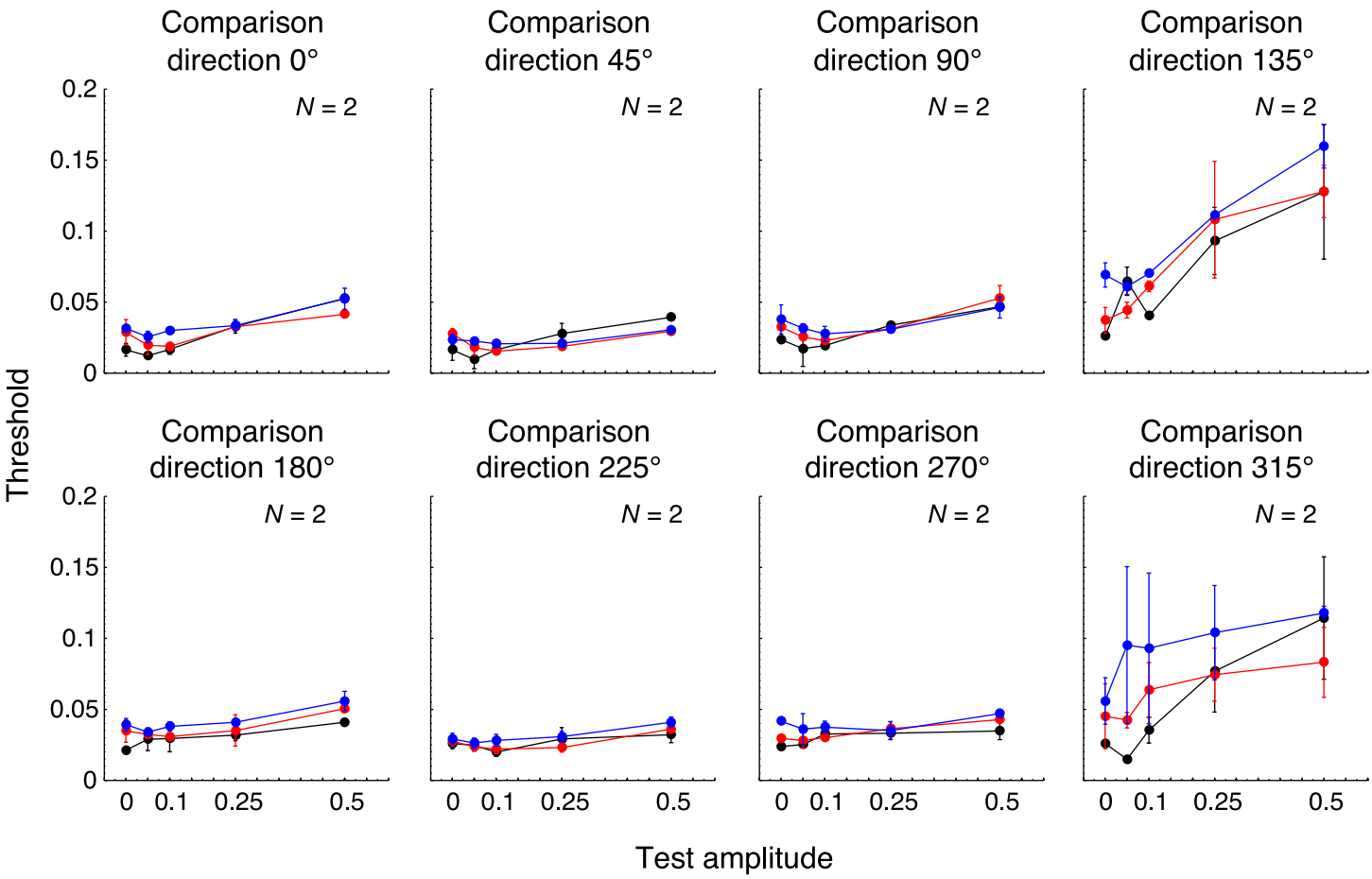

Figure 12. Discrimination thresholds for test direction 315° separately for each of eight comparison directions at the adaptation point (test amplitude of zero) and at test locations away from the adaptation point for the disk (black), pink noise 0.25 (red), and pink noise 0.5 (blue). Filled symbols indicate thresholds for the particular test location averaged across two observers (D.P. and M.G.). Error bars show the standard error of the mean.

elevated threshold at this test location. Two of the observers were made aware of this situation and instructed to avoid this response behavior. Their TvC functions showed a less pronounced peak at this test location although it was still present. Figure 12 shows that the shift away from the adaptation point in the test direction 315° affected only the thresholds in the direction of the shift. This speaks against a cardinal model of color discrimination and for the existence of mechanisms tuned to intermediate directions.

These results can be interpreted as being determined by two noise components. One of these is due to the variation of chromaticities in the stimulus, and the other one is due to the distance of the test stimuli from the adaptation point.

Extended model predictions

In addition to the data presented in Figure 4, we also fitted the model to the discrimination data for the stimuli with chromatic variation along the first diagonal presented in Figure 7 and to the data shown in Figures 9 and 11. The data presented here were collected using a different setup and slightly modified methods compared with the previous experiments. Since Figure 1 shows that the discrimination ellipses for the disk at the adaptation point were similar for the two setups, we pooled the previous and the new data. Altogether, the model was fitted to 528 data points. Table 3 depicts the values of the model parameters for the fit to the extended data set.

The inclusion of the new data into the data set to which the model was fitted changed the parameters of the model considerably. The change was more pronounced for the eight mechanisms model. The four mechanisms model was less affected presumably because the two orthogonal chromatic distributions cause similar excitation of the cardinal mechanisms. Compared with the tuning widths in Table 1, the cardinal mechanisms in the four mechanisms model—with the exception of the mechanism at 90°—were more narrowly tuned, whereas the cardinal mechanisms in the eight mechanisms model fitted to the extended data set were more broadly tuned than before.

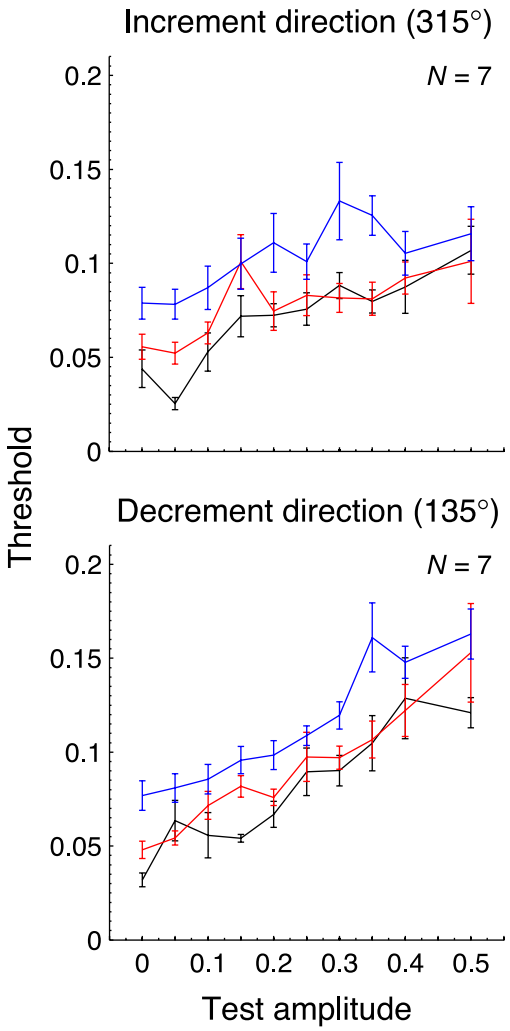

Figure 13. Increment comparison direction (315°) discrimination thresholds (left) and decrement comparison direction (135°) discrimination thresholds (right) for test direction 315° at 10 test locations (0, 0.05, 0.1, 0.15, 0.2, 0.25, 0.3, 0.35, 0.4, 0.5) for the disk (black), pink noise 0.25 (red), and pink noise 0.5 (blue). Filled symbols indicate thresholds averaged across seven observers (C.H., D.K., D.P., M.G., M.O., N.L., S.B.). Error bars show standard error of the mean.

	$M = 4$	$M = 8$
Response function		
g	21.964	17.810
p	0.552	0.562
Tuning width (HWHH)		
k_0	45.613	58.162
k_{45}	–	57.032
k_{90}	63.194	70.832
k_{135}	–	52.168
k_{180}	49.524	61.585
k_{225}	–	61.239
k_{270}	35.464	50.873
k_{315}	–	46.648
Sensitivity		
s_0	22.008	10.751
s_{45}	–	24.745
s_{90}	18.741	9.678
s_{135}	–	12.228
s_{180}	16.958	7.841
s_{225}	–	20.343
s_{270}	25.984	21.325
s_{315}	–	22.228

Table 3. Parameters for the model with four and the model with eight mechanisms. g and p are the parameters of the response function, k_i is the tuning width of the sensitivity function given as half-width at half-height (HWHH), and s_i is the sensitivity of the ith mechanism.

The mechanisms on the second diagonal (135° and 315°) were still more narrowly tuned than the other mechanisms, but the differences were smaller than in the previous fit. The sensitivity parameters were again lower for the mechanisms in the upper two quadrants.

Both Akaike's information criterion and the Bayesian information criterion show an advantage of the model with eight mechanisms compared with the model with four mechanisms (Tables 4 and 5). In addition, we also fitted eight mechanisms models setting either k or s to one for all mechanisms. In a third variant, only the parameters of the response function g and p were fitted and both k and s were set to one for all mechanisms. The good performance of the variant in which the tuning width parameters were set to one is not surprising considering that they were close to one even when they were included in the fit. While AIC favored the variant where both the parameters k and s were fitted, BIC favored the variants where either k or s was fitted over the full model. However, both information criteria favored all variants of the eight mechanisms model over the four mechanisms model. We also tested a model with six mechanisms. This model had two mechanisms on the second diagonal (135° and 315°) in addition to mechanisms at the cardinal directions. This

M	Parameter	RSS	K	AIC_c	ΔAIC_c
8	g, p, $k_{1:8}$, $s_{1:8}$	53.714	18	−1169.4	0
8	g, p, $k_{1:8}$	56.383	10	−1160.7	8.69
8	g, p, $s_{1:8}$	58.986	10	−1136.8	32.51
8	g, p	65.999	2	−1093.9	75.43
6	g, p, $k_{1:6}$, $s_{1:6}$	71.139	14	−1029.5	139.82
4	g, p, $k_{1:4}$, $s_{1:4}$	74.172	10	−1015.9	153.48

Table 4. Evaluation of the model variants using Akaike's information criterion (AIC_c). M gives the number of mechanisms in the model, RSS is the residual sum of squares, K the number of parameters in the model, AIC_c is the information criterion as defined by Equation 5, and ΔAIC_c was computed as the difference between AIC_c and $\min(AIC_c)$.

M	Parameter	RSS	*K*	BIC	ΔBIC
8	g, p, $k_{1:8}$	56.383	10	−1118.4	0
8	g, p, $s_{1:8}$	58.986	10	−1094.6	23.83
8	g, p, $k_{1:8}$, $s_{1:8}$	53.714	18	−1093.9	24.55
8	g, p	65.999	2	−1085.4	32.99
4	g, p, $k_{1:4}$, $s_{1:4}$	74.172	10	−973.6	144.79
6	g, p, $k_{1:6}$, $s_{1:6}$	71.139	14	−970.6	147.82

Table 5. Evaluation of the model variants using the Bayesian information criterion (BIC). *M* gives the number of mechanisms in the model, *RSS* is the residual sum of squares, *K* the number of parameters in the model, BIC is the information criterion as defined by Equation 6, and ΔBIC was computed as the difference between BIC and min(BIC).

model produced only a slightly improved fit compared with the four mechanisms model. ΔBIC is smaller for the four mechanisms model, while ΔAIC_c is smaller for the six mechanisms model.

The finding that even the eight mechanisms model with both the parameters k and s set to one for all mechanisms provided a better fit to the data than the four mechanisms model variant where both parameters were fitted for each mechanism is presumably based on the fact that the eight mechanisms model can predict elongated ellipses at the adaptation point and ellipses elongated in intermediate directions mainly as a consequence of the additional mechanisms along the intermediated directions, whereas the four mechanisms model requires at least some of its mechanisms to be more narrowly tuned than 60° to predict these ellipses. We also fitted different variants of the four mechanisms model to the data. Fitting a four mechanisms model where only the parameters of the response function were fitted and both k and s were set to one for all mechanisms produced circular ellipses at the adaptation point and at intermediate test directions. If the parameter s was fitted separately for each mechanism, while all tuning width parameters were still set to one, the ellipses at

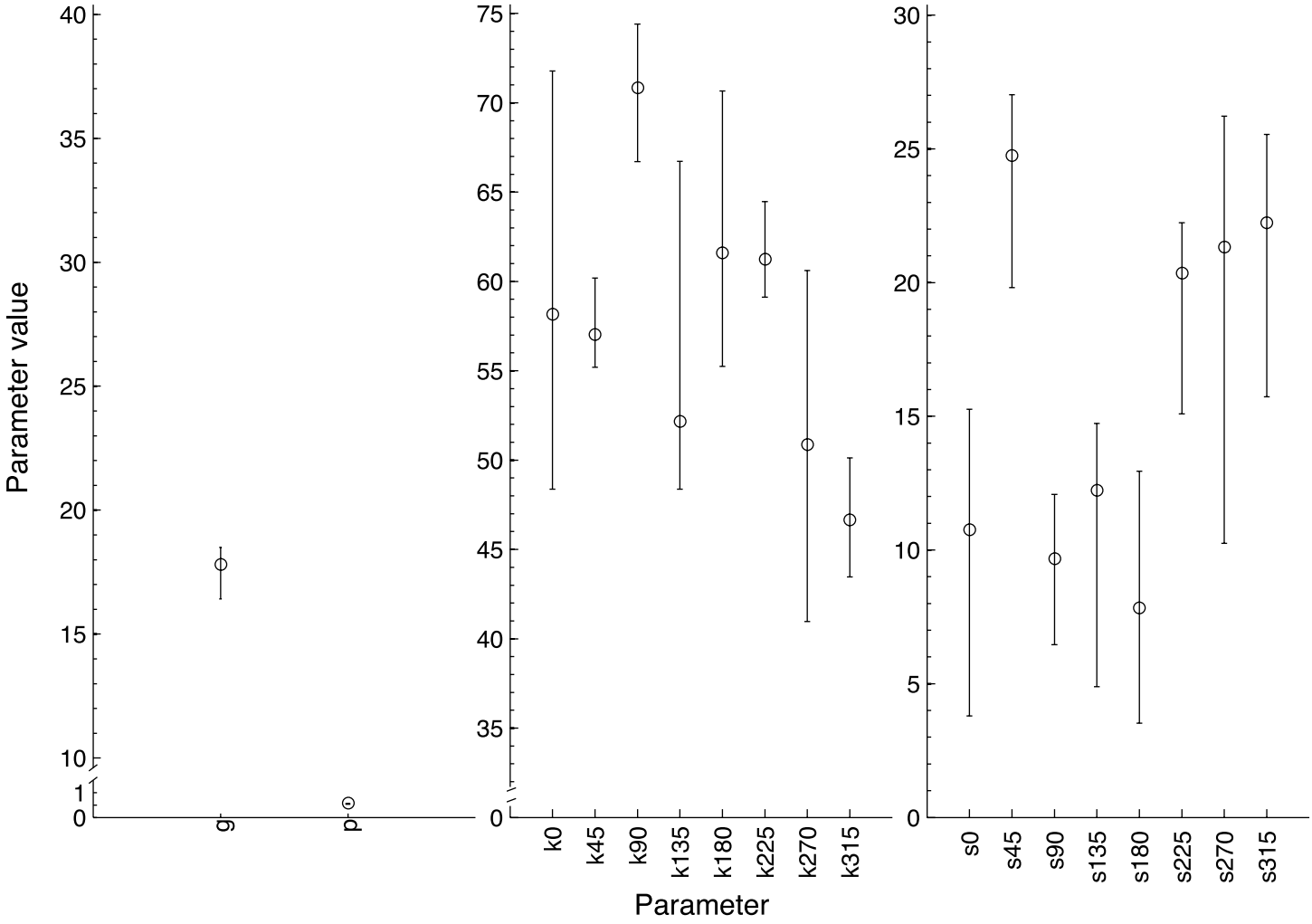

Figure 14. The 95% confidence intervals for the 18 parameters of the eight mechanisms model based on 1500 bootstrap fits. The *x*-axis shows the different parameters, and the *y*-axis shows the values of the parameters. Error bars show 95% confidence intervals around the parameter values in Table 3 (open symbols). The values of k_i are given as HWHH.

intermediate test directions showed an elongation in the direction of the mechanisms with the lower sensitivity parameter. When the tuning width parameters were fitted and the parameter s was set to one for all mechanisms, the model could predict the effect of the chromatic distributions at the adaptation point and ellipses elongated in intermediate test directions.

We applied a bootstrap procedure to compute 95% confidence intervals for the 18 parameters of the eight mechanisms model. For each threshold averaged across the observers, we computed the standard deviation. This standard deviation was then used to generate a normal distribution around each of the thresholds. From this distribution, new thresholds were randomly picked to generate the bootstrap data sets. The model was fitted to the new data sets, and 95% confidence intervals were computed for the resulting parameter values of 1500 bootstrap fits. For each bootstrap, a new set of images was generated. The results are shown in Figure 14.

There was little variation in the values of the response function parameters g and p. The tuning width parameters k_i varied to a larger extend. With the exception of the mechanism at 315° which was significantly more narrowly tuned and the mechanism at 90° which was significantly more broadly tuned, the tuning widths of the other mechanisms were not significantly different from an HWHH of 60°. There also was wide variation in the confidence intervals of the sensitivity parameters s_i, but the parameters fall into two groups. The higher sensitivity values for the mechanisms in the lower two quadrants (225°, 270°, 315°) are in accordance with the lower discrimination thresholds in this region. The high sensitivity value for the mechanism at 45° was not directly related to the data, since discrimination thresholds for this direction were comparatively high. But a simple interpretation of the parameter values might not be adequate because the thresholds depend not only on the parameter values of the mechanism itself but also on the properties of the adjacent mechanisms.

Based on the 1500 bootstraps, we have computed the correlations among the parameters. Most correlations were small (around $r = 0.5$ or clearly lower). The parameters of the response function g and p were highly correlated ($r = 0.81$). There was a tendency of higher negative correlations between the parameters k_i and s_i. This means that more narrow tuning leads to a higher value of the sensitivity parameter s. This was especially pronounced for the mechanism at 225° ($r = 0.75$).

Figure 15 depicts the predictions of models with four and eight mechanisms to the averaged discrimination data for stimuli chromatically variegated along the first diagonal (cf. Figure 7).

For stimuli with chromatic variation along the first diagonal differences between the two model variants were smaller than for stimuli with chromatic variation along the second diagonal. Since the ellipses at intermediate test directions for the stimuli chromatically variegated along the first diagonal were less elongated, they could be more accurately predicted by the four mechanisms model than the narrow ellipses for stimuli chromatically variegated along the second diagonal.

The major advantage of the model with eight mechanisms can be seen in Figure 16 where the area and eccentricity of the predicted discrimination ellipses for all three types of stimuli are plotted separately for the two model variants.

The main difference between the two model variants is visible at the intermediate test locations (45°, 135°, 225°, 315°). At these test locations, the model with four mechanisms predicted discrimination ellipses for the two types of chromatically variegated stimuli that were almost similar in both area and eccentricity. This is most obvious at test locations 135° and 315° where the four mechanisms

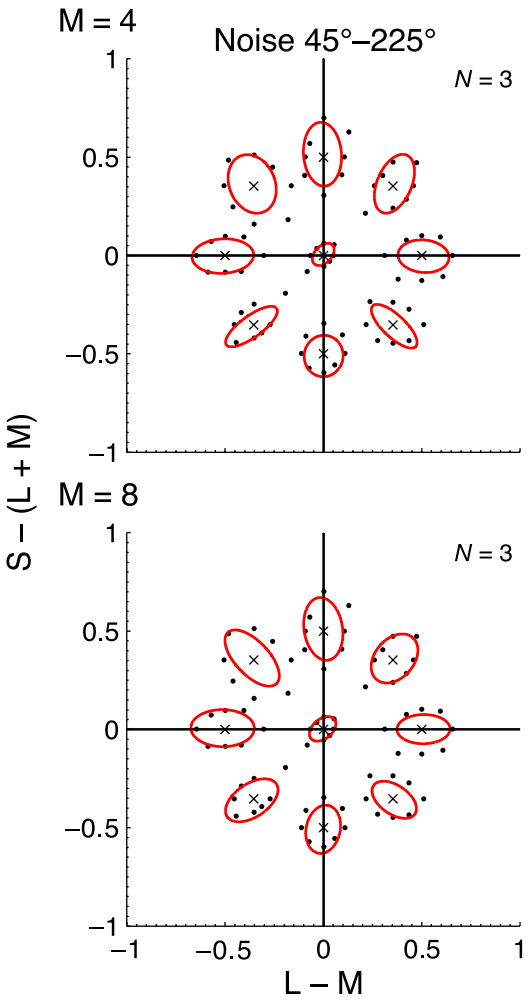

Figure 15. Discrimination thresholds (black dots) at the adaptation point and at test locations away from the adaptation point for stimuli with chromatic variation along the first diagonal averaged across three observers (C.H., D.P.E., M.G.). Ellipses show discrimination contours predicted by a model with four mechanisms (top) and by a model with eight mechanisms (bottom). Crosses indicate the chromaticities at the test location.

model did not predict the narrow ellipses for the stimuli with chromatic variation along the second diagonal and the more rounded ellipses for stimuli with chromatic variation along the first diagonal. On the intermediate test directions, ellipses for all stimuli were more rounded in the upper two quadrants and more elongated in the lower two quadrants. The eight mechanisms model on the contrary predicted the interaction between chromatic distributions and test locations on the intermediate axes. Discrimination ellipses were more elongated, and the area was smaller when the chromatic distribution was collinear to the test direction and more rounded and larger when it was orthogonal to the test direction.

Figure 17 shows the model fits to the discrimination data presented in Figure 9.

The predictions were not so accurate for this data set as they were for the other data sets especially for test amplitudes between the adaptation point and the highest test amplitude (0.5). This is partly due to the use of stimuli with an amplitude spectrum similar to $1/f$. Thresholds for these stimuli were slightly lower than thresholds for stimuli with an amplitude spectrum similar to $1/f^2$. The model that does not account for the spatial frequency of the stimuli provides a better fit to the thresholds for the $1/f^2$ stimuli. Moreover, the majority of data points were measured at test locations with a test amplitude of 0.5. This might have favored fits to these data points. Chen et al. (2000a, 2000b) showed that a simple power function as the one used in our model is not optimal to describe TvC functions. Here, the focus was on predicting the interplay between the effect of chromatic distributions and the effect of pedestal contrast. The model correctly predicted the rotation of the discrimination ellipses away from an elongation in the direction of the chromatic distribution toward an elongation in the direction of the shift away from the adaptation point. It also shows that this happened

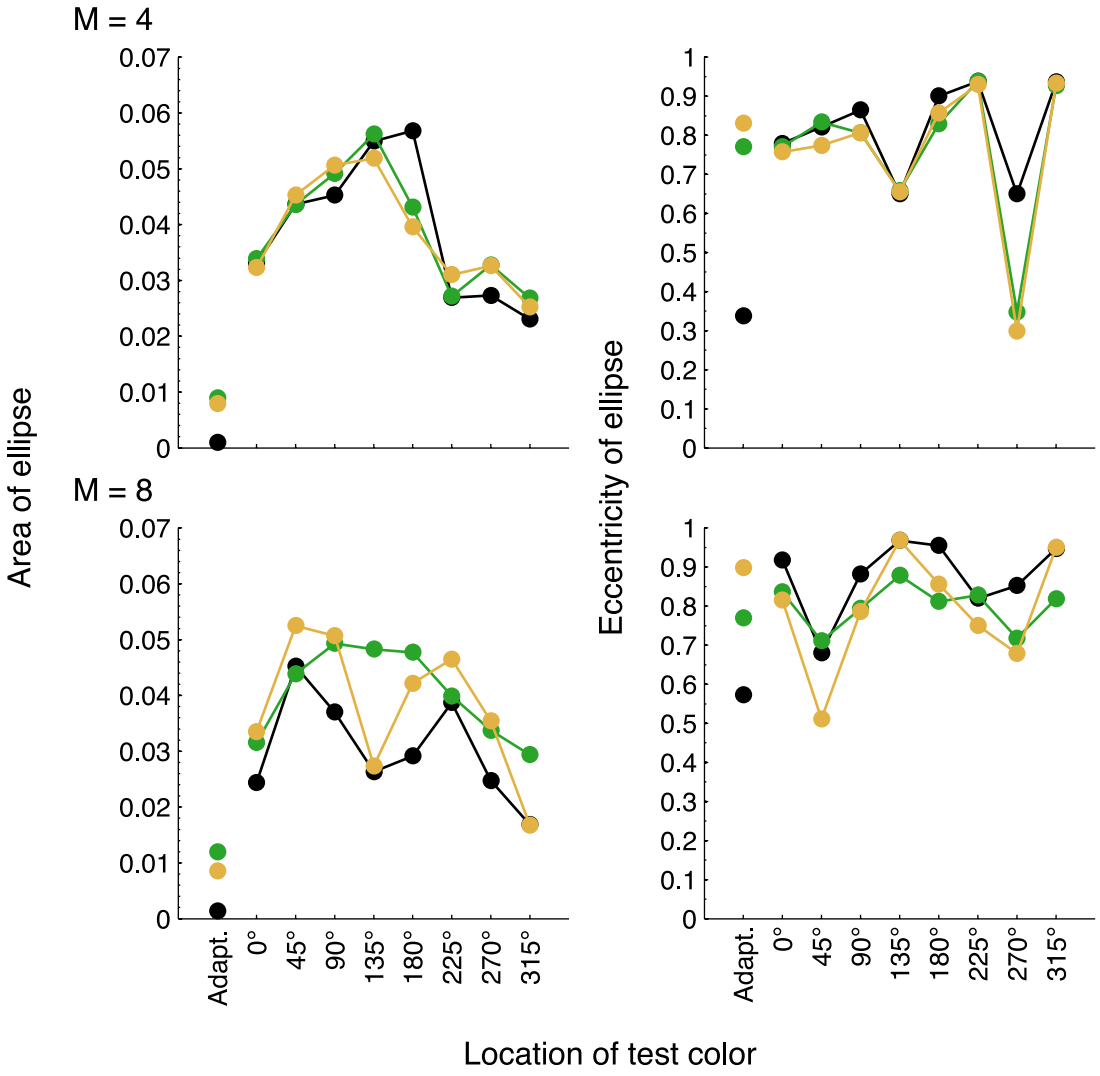

Figure 16. Area (first column) and eccentricity (second column) of the discrimination ellipses predicted by a model with four mechanisms (first row) and by a model with eight mechanisms (second row) for the disk (black), stimuli chromatically variegated along the first diagonal (green), and stimuli chromatically variegated along the second diagonal (yellow).

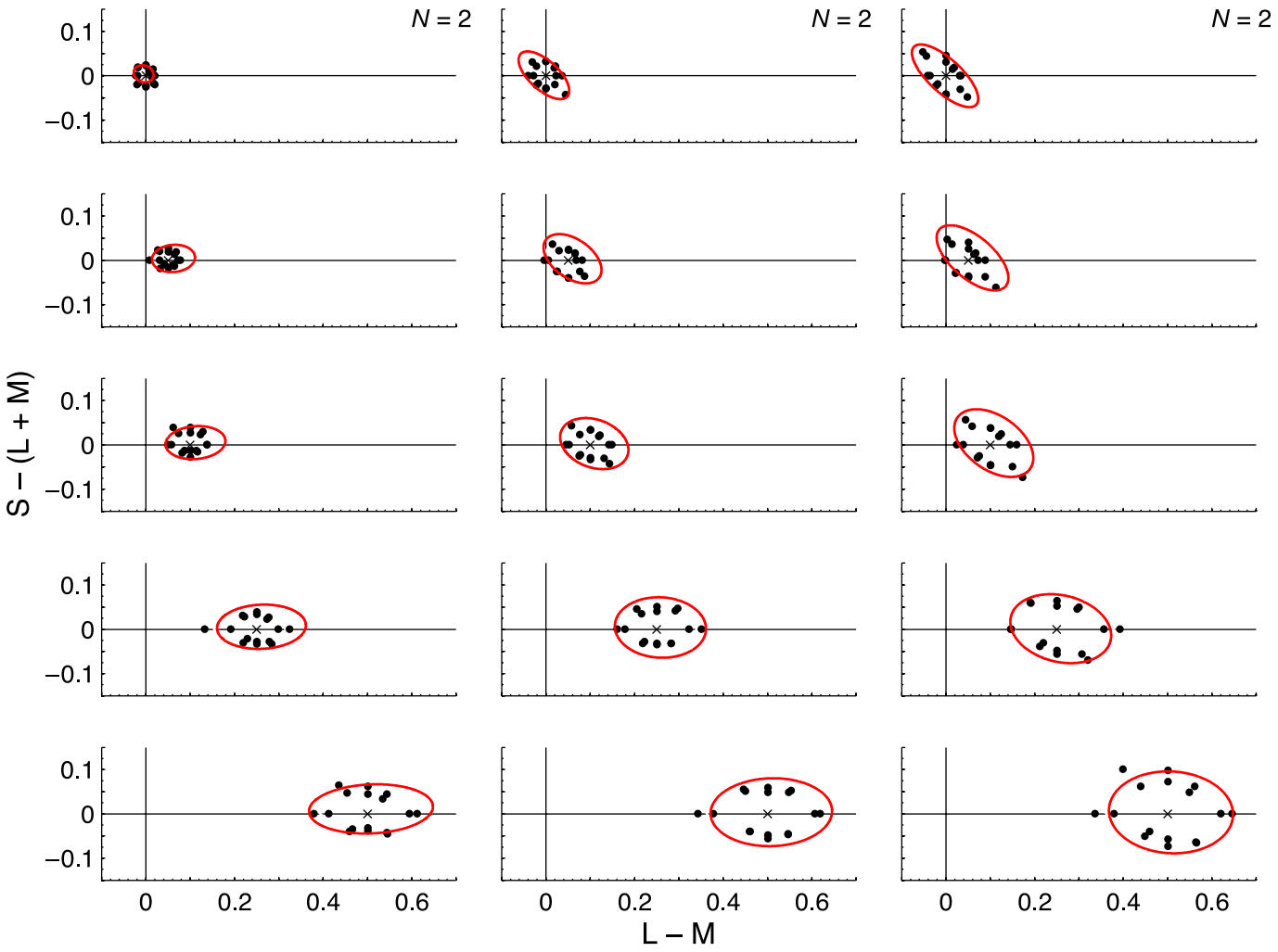

Figure 17. Discrimination thresholds of two observers (black symbols) for test direction 0° at the adaptation point and at four test locations away from the adaptation point (rows from top to bottom: 0, 0.05, 0.1, 0.25, and 0.5) for the disk (first column), pink noise 0.25 (second column), and pink noise 0.5 (third column). Ellipses show model predictions from a model with eight mechanisms based on the fit to all data sets. Crosses indicate the chromaticities at the test location.

at a lower test amplitude for the stimulus with the lower chromatic amplitude.

Considering the basic geometry of the model, one could hypothesize that thresholds in the test direction should outweigh thresholds in the direction of the chromatic distribution when the test amplitude is equal to the amplitude of the chromatic distribution, i.e., when the distribution is completely shifted to one side of the adaptation point because from this point on the activation of most mechanisms is the same for a chromatically variegated stimulus and a homogeneously colored stimulus of the same size at least if the distribution of chromaticities is symmetric. Figure 9 shows that the discrimination ellipse for the pink noise stimulus with the lower amplitude is already elongated in the test direction at a test amplitude of 0.25. The actual test amplitude at which the ellipse rotates might be influenced by the chromatic histogram of the stimulus. As said above, the chromaticities of the pink noise stimuli were approximately normally distributed. This means that 95% of the chromaticities were within two standard deviations of the distribution. The activation caused by the remaining 5% might be negligible. In this case, the ellipse would start to rotate into the test direction before the test amplitude equals the amplitude of the chromatic distribution.

General discussion

Experimental results

We measured chromatic discrimination thresholds for homogeneously colored stimuli and chromatically variegated stimuli. The chromaticities of these stimuli varied either along the first or along the second diagonal in DKL color space. We found an elongation of the discrimination

ellipses in the direction of the chromatic distribution at the adaptation point for the chromatically variegated stimuli, and a differential effect at test locations away from the adaptation point depending on whether the test direction was orthogonal or collinear to the direction of the chromatic distribution. TvC functions for homogeneous and variegated stimuli showed that discrimination thresholds can be thought of as mediated by two components. One component is due to the chromatic distribution, and the other one is due to the distance from the adaptation point. At a certain test amplitude, the component due to the distance from the adaptation point outweighs the effect of the chromatic distribution which renders the discrimination ellipses for the variegated stimuli similar to the ellipses for the homogeneous stimuli. Together with the data presented in Hansen et al. (2008) these data suggest that chromatic discrimination is mediated by more than four cardinal mechanisms. To substantiate this, we outlined a chromatic discrimination model with multiple chromatic mechanisms.

The chromaticities of the chromatically variegated stimuli we used here and in Hansen et al. (2008) only varied along a line on the first or second diagonal. This was motivated by our goal to investigate the existence of mechanisms intermediate to the cardinal axes. Although these chromatic distributions represent an improvement in naturalness compared with homogeneously colored stimuli, they are still quite artificial. In Hansen et al., we also measured discrimination thresholds for photographs of natural objects. The chromatic distributions of these objects had an approximately elliptical shape with the major chromatic variation along one direction and minor variation in other directions. Since we found no differences between discrimination thresholds for the natural objects and synthetic stimuli with chromatic variation only in one direction, the synthetic stimuli might be an acceptable approximation of objects where the chromatic variation in directions orthogonal to the major variation is comparatively small.

Model evaluation

Fitting the model to the data presented here and in Hansen et al. (2008) showed that a discrimination model based on the vector differences between the activations of chromatic mechanisms accounted for thresholds for stimuli with a chromatic distribution. We also showed that a model with eight mechanisms performed better than a model with four mechanisms. The strongest evidence for the eight mechanisms model is that the model with four mechanisms predicted identical thresholds for the two types of chromatic distributions for test locations on the oblique axes. Basic geometrical considerations show that the excitation of the two cardinal mechanisms, which are activated by these stimuli at the intermediate test locations, should be the same for both types of chromatic distributions. This cannot be compensated by adjusting the tuning widths and sensitivities of the mechanisms in the fitting procedure. Table 3 shows that a model with four mechanisms requires the mechanisms to be more narrowly tuned than expected from a linear combination of cone inputs whereas the model with eight mechanisms had broadly tuned mechanisms along the cardinal axes and along the first diagonal. Mechanisms along the second diagonal were more narrowly tuned. However, the deviations from a linear combination of cone inputs were small. Even when the tuning width parameters were set to unity for all mechanisms, the eight mechanisms model predicted the effect of the chromatic distributions at the adaptation point and the ellipses elongated in intermediate test directions.

The model performed less well in predicting the form of the TvC function. The non-monotonic TvC function cannot be accurately described by the power function that we used as response function. As shown by Foley (1994) and Foley and Chen (1997) in the luminance domain and by Chen et al. (2000a, 2000b) for chromatic discrimination, an inhibitory term in the response function is required to model TvC functions. We also tested response functions with inhibitory parts similar to those described by Chen et al. (2000a, 2000b). These response functions provided no increase in the accuracy of the fits but the predictions were less stable, so that not all thresholds could be predicted simultaneously. We do not claim that an inhibitory part of the response function is dispensable. The reason that the power function did well might be that the majority of our data points were at intermediate contrast levels where the power function provides a good description of the increase in thresholds. Here, the model was reduced to its essential components to provide an easily interpretable fit to the data in terms of the number and properties of chromatic mechanisms. We are planning to refine the model in the future to make it applicable to more general question, e.g., the evaluation of image quality.

One feature that distinguishes the model outlined here from the similar models proposed by Chen et al. (2000b), D'Zmura and Knoblauch (1998), Goda and Fujii (2001), and Hansen and Gegenfurtner (2006) is that we fitted the tuning width and sensitivity of each mechanism separately. This was motivated by the finding that discrimination ellipses differed in size and elongation at the different test locations away from the adaptation point. Namely, ellipses in the upper two quadrants were in general larger than in the lower two quadrants, and ellipses on the first diagonal were more rounded than on the second diagonal. The results of the bootstrap procedure showed that a model with eight broadly tuned mechanisms does provide a good approximation to the tuning of the mechanisms. This is in accordance with Hansen and Gegenfurtner (2006) who found that a model with multiple broadly tuned mechanisms accounted for detection in a noise-masking paradigm. The differences between the two intermediate axes require differently tuned mechanisms. This is reflected by the more narrowly

tuned mechanisms along the second diagonal. It should be noted that the direction of this diagonal is also the direction in which the chromaticities of most natural objects and natural scenes have their major chromatic variation (Webster & Mollon, 1997). It could be hypothesized that these mechanisms are tuned to processes especially these chromatic variations.

Allowing differently tuned and weighted mechanisms was also necessary to investigate whether the four mechanisms model is in principle able to account for the data for the two chromatic distributions. We found that the four mechanisms model accounted for ellipses elongated in the direction of the chromatic distribution at the adaptation point and ellipses elongated in intermediate directions away from the adaptation point only if at least some mechanisms were narrowly tuned. The model fits revealed that the mechanisms in the four mechanisms model cannot be tuned in such a way that it could predict the different discrimination ellipses for the two types of chromatic distributions at intermediate test locations.

Image quality models

Existing image quality and image similarity models (Ahumada, 1993; Daly, 1993; Lovell, Párraga, Troscianko, Ripamonti, & Tolhurst, 2006; Neumann & Gegenfurtner, 2006; Tolhurst, Ripamonti, Párraga, Lovell, & Troscianko, 2005; Zhang & Wandell, 1996, 1998) are based on the computation of the pixel-by-pixel differences of two images for different spatial frequency channels.

S-CIELAB (Zhang & Wandell, 1996, 1998) is a spatial extension to the CIELAB color metric designed to quantify color reproduction errors of digital images. It is an improvement compared with the CIELAB metric in that it takes into account the spatial sensitivity of the human visual system. To compute the S-CIELAB metric, the images are converted into a color opponent representation. In the next step, the resulting three image planes are processed for each image in such a way that the three planes are weighted with the spatial sensitivity to the color dimension represented by each plane. The filtered images are then converted into the CIELAB color space. Differences between two images are computed pixel-by-pixel using the CIELAB difference formula.

Contrary to the CIELAB metric, S-CIELAB predicts different visibility of color differences for textured images and for homogeneously colored images. Discriminability is determined by the different sensitivities to different color directions implemented in the CIELAB transformation and by the different spatial sensitivities introduced by the spatial extension to CIELAB. S-CIELAB might predict different visibility for shifts of a chromatic distribution into different directions, but these differences depend on the different chromatic and spatial sensitivities and not on the chromatic distribution itself. Due to the use of the pixel-by-pixel differences, this metric does not distinguish between, for example, a shift into the direction of the chromatic distribution and a shift into the orthogonal direction. We showed that chromatic distributions affect chromatic discrimination thresholds in a considerable manner. This effect should be taken into account when measuring image quality or when defining norms. However, existing models might be modified by using a difference metric that accounts for the variation of chromaticities (e.g., Mahalanobis distance).

Conclusion

We showed that chromatic discrimination thresholds for chromatically variegated stimuli can be modeled using a model which is based on the responses of the second stage cone-opponent mechanisms. The model accounts both for the effects of chromatic distributions and pedestal contrast. A model with eight mostly broadly tuned mechanisms provided a better fit to the data than a model with four mechanisms.

Acknowledgments

This research was supported by the German Science Foundation grant Ge 879/5.

Commercial relationships: none.
Corresponding author: Martin Giesel.
Email: Martin.Giesel@psychol.uni-giessen.de.
Address: Justus-Liebig-Universität Giessen, Abteilung Allgemeine Psychologie, Otto-Behaghel-Str. 10F, 35394 Giessen, Germany.

References

Ahumada, A. J. (1993). Computational image quality metrics: A review. *SID Digest of Technical Papers, 24,* 305–308.

Akaike, H. (1974). A new look at the statistical model identification. *IEEE Transactions on Automatic Control, 19,* 716–723.

Boynton, R. M., & Kambe, N. (1980). Chromatic difference steps of moderate size measured along theoretically critical axes. *Color Research and Application, 5,* 137–23.

Brainard, D. H. (1997). The Psychophysics Toolbox. *Spatial Vision, 10,* 433–436. [PubMed]

Burnham, K. P., & Anderson, D. R. (2002). *Model selection and multimodel inference: A practical information-theoretical approach* (2nd ed.). New York: Springer Verlag.

Burnham, K. P., & Anderson, D. R. (2004). Multimodel inference: Understanding AIC and BIC in model selection. *Sociological Methods and Research, 33,* 261–304.

Chen, C.-C., Foley, J. M., & Brainard, D. H. (2000a). Detection of chromoluminance patterns on chromoluminance pedestals I: Threshold measurements. *Vision Research, 40,* 773–788. [PubMed]

Chen, C.-C., Foley, J. M., & Brainard, D. H. (2000b). Detection of chromoluminance patterns on chromoluminance pedestals II: Model. *Vision Research, 40,* 789–803. [PubMed]

Cottaris, N. P., & De Valois, R. L. (1998). Temporal dynamics of chromatic tuning in macaque primary visual cortex. *Nature, 395,* 896–900. [PubMed]

Daly, S. (1993). Digital images and human vision. In A. B. Watson (Ed.), *The visible difference predictor: An algorithm for the assessment of image fidelity* (pp. 179–206). Cambrigde, MA: MIT Press.

Derrington, A. M., Krauskopf, J., & Lennie, P. (1984). Chromatic mechanisms in lateral geniculate nucleus of macaque. *The Journal of Physiology, 357,* 241–265. [PubMed] [Article]

D'Zmura, M. (1991). Color in visual search. *Vision Research, 31,* 951–966. [PubMed]

D'Zmura, M., & Knoblauch, K. (1998). Spectral bandwidths for the detection of color. *Vision Research, 38,* 3117–3128. [PubMed]

Field, D. J. (1989). What the statistics of natural images tell us about visual coding. *Proceedings of SPIE, 1077,* 269–276.

Foley, J. M. (1994). Human luminance pattern-vision mechanisms: Masking experiments require a new model. *Journal of the Optical Society of America A, Optics, Image Science, and Vision, 11,* 1710–1719. [PubMed]

Foley, J. M., & Chen, C.-C. (1997). Analysis of the effect of pattern adaptation on pattern pedestal effects: A two-process model. *Vision Research, 37,* 2779–2788. [PubMed]

Gegenfurtner, K. R., & Kiper, D. C. (1992). Contrast detection in luminance and chromatic noise. *Journal of the Optical Society of America A, Optics and Image Science, 9,* 1880–1888. [PubMed]

Gegenfurtner, K. R., Kiper, D. C., & Levitt, J. B. (1997). Functional properties of neurons in macaque area V3. *Journal of Neurophysiology, 77,* 1906–1923. [PubMed] [Article]

Goda, N., & Fujii, M. (2001). Sensitivity to modulation of color distribution in multicolored textures. *Vision Research, 41,* 2475–2485. [PubMed]

Graham, N. V. S. (1989). *Visual pattern analyzers* (Oxford Psychology Series). New York: Oxford University Press.

Grassmann, H. (1853). Zur Theorie der Farbenmischung. *Annalen der Physik, 89,* 69.

Guth, S. L., Massof, R. W., & Benzschawel, T. (1980). Vector model for normal and dichromatic color vision. *Journal of the Optical Society of America, 70,* 197–212. [PubMed]

Halíř, R., & Flusser, J. (1998). Numerically stable direct least squares fitting of ellipses. In *Proceedings of the 6th International Conference in Central Europe on Computer Graphics and Visualization* (pp. 125–132). Czech Republic: Plzen.

Hansen, T., & Gegenfurtner, K. R. (2005). Classification images for chromatic signal detection. *Journal of the Optical Society of America A, Optics, Image Science, and Vision, 22,* 2081–2089. [PubMed]

Hansen, T., & Gegenfurtner, K. R. (2006). Higher level chromatic mechanisms for image segmentation. *Journal of Vision, 6*(3):5, 239–259, http://journalofvision.org/6/3/5/, doi:10.1167/6.3.5. [PubMed] [Article]

Hansen, T., Giesel, M., & Gegenfurtner, K. R. (2008). Chromatic discrimination of natural objects. *Journal of Vision, 8*(1):2, 1–19, http://journalofvision.org/8/1/2/, doi:10.1167/8.1.2. [PubMed] [Article]

Hansen, T., Olkkonen, M., Walter, S., & Gegenfurtner, K. R. (2006). Memory modulates color appearance. *Nature Neuroscience, 9,* 1367–1368. [PubMed]

Helmholtz, H. v. (1896). *Handbuch der physiologischen Optik* (2nd ed.). Hamburg: Voss.

Jameson, D., & Hurvich, L. M. (1955). Some quantitative aspects of an opponent colors theory—I. Chromatic responses and spectral saturation. *Journal of the Optical Society of America, 45,* 546.

Johnson, E. N., Hawken, M. J., & Shapley, R. (2001). The spatial transformation of color in the primary visual cortex of the macaque monkey. *Nature Neuroscience, 4,* 409–416. [PubMed]

Johnson, E. N., Hawken, M. J., & Shapley, R. (2004). Cone inputs in macaque primary visual cortex. *Journal of Neurophysiology, 91,* 2501–2514. [PubMed] [Article]

Judd, D. B. (1951). Report on US secretariat committee on colorimetry and artificial daylight. In *Proceedings of the Twelfth Session of the CIE, Stockholm, Sweden* (p. 11). Paris, France: Bureau Central de la CIE.

Kingdom, F. A. A. (2008). Perceiving light versus material. *Vision Research, 48,* 2090–2105. [PubMed]

Kiper, D. C., Fenstemaker, S. B., & Gegenfurtner, K. R. (1997). Chromatic properties of neurons in macaque area V2. *Visual Neuroscience, 14,* 1061–1072. [PubMed]

Knoblauch, K., & Maloney, L. T. (1996). Testing the indeterminacy of linear color mechanisms from color discrimination data. *Vision Research, 36,* 295–306. [PubMed]

Koenderink, J. J., van de Grind, W. A., & Bouman, M. A. (1972). Opponent color coding: A mechanistic model and a new metric for color space. *Kybernetik, 10,* 78–98. [PubMed]

Komatsu, H. (1998). Mechanisms of central color vision. *Current Opinion in Neurobiology, 8,* 503–508. [PubMed]

Komatsu, H., Ideura, Y., Kaji, S., & Yamane, S. (1992). Color selectivity of neurons in the inferior temporal cortex of the awake macaque monkey. *Journal of Neuroscience, 12,* 408–424. [PubMed] [Article]

Krauskopf, J. (1980). Discrimination and detection of changes in luminance. *Vision Research, 20,* 671–677. [PubMed]

Krauskopf, J., & Gegenfurtner, K. (1992). Color discrimination and adaptation. *Vision Research, 32,* 2165–2175. [PubMed]

Krauskopf, J., Williams, D. R., & Heeley, D. W. (1982). Cardinal directions of color space. *Vision Research, 22,* 1123–1131. [PubMed]

Krauskopf, J., Williams, D. R., Mandler, M. B., & Brown, A. M. (1986). Higher order color mechanisms. *Vision Research, 26,* 23–32. [PubMed]

Krauskopf, J., Wu, H. J., & Farell, B. (1996). Coherence, cardinal directions and higher-order mechanisms. *Vision Research, 36,* 1235–1245. [PubMed]

Krauskopf, J., Zaidi, Q., & Mandler, M. B. (1986). Mechanisms of simultaneous color induction. *Journal of the Optical Society of America A, Optics and Image Science, 3,* 1752–1757. [PubMed]

Legge, G. E. (1981). A power law for contrast discrimination. *Vision Research, 21,* 457–467. [PubMed]

LeGrand, Y. (1968). *Light, colour and vision*. London: Chapman & Hall.

Lennie, P., Krauskopf, J., & Sclar, G. (1990). Chromatic mechanisms in striate cortex of macaque. *Journal of Neuroscience, 10,* 649–669. [PubMed] [Article]

Levitt, H. (1971). Transformed up-down methods in psychoacoustics. *Journal of the Acoustical Society of America, 49,* 467–477. [PubMed]

Li, A., & Lennie, P. (1997). Mechanisms underlying segmentation of colored textures. *Vision Research, 37,* 83–97. [PubMed]

Lindsey, D. T., & Brown, A. M. (2004). Masking of grating detection in the isoluminant plane of DKL color space. *Visual Neuroscience, 21,* 269–273. [PubMed]

Lovell, P. G., Párraga, C. A., Troscianko, T., Ripamonti, C., & Tolhurst, D. J. (2006). Evaluation of a multiscale color model for visual difference prediction. *ACM Transactions on Applied Perception, 3,* 155–178.

MacLeod, D. I., & Boynton, R. M. (1979). Chromaticity diagram showing cone excitation by stimuli of equal luminance. *Journal of the Optical Society of America, 69,* 1183–1186. [PubMed]

Mizokami, Y., Paras, C., & Webster, M. A. (2004). Chromatic and contrast selectivity in color contrast adaptation. *Visual Neuroscience, 21,* 359–363. [PubMed]

Monaci, G., Menegaz, G., Süsstrunk, S., & Knoblauch, K. (2004). Chromatic contrast detection in spatial chromatic noise. *Visual Neuroscience, 21,* 291–294. [PubMed]

Neumann, D., & Gegenfurtner, K. R. (2006). Image retrieval and perceptual similarity. *ACM Transactions on Applied Perception, 3,* 31–47.

Noorlander, C., & Koenderink, J. J. (1983). Spatial and temporal discrimination ellipsoids in color space. *Journal of the Optical Society of America, 73,* 1533–1543. [PubMed]

Pelli, D. G. (1997). The VideoToolbox software for visual psychophysics: Transforming numbers into movies. *Spatial Vision, 10,* 437–442. [PubMed]

Poirson, A. B., Wandell, B. A., Varner, D. C., & Brainard, D. H. (1990). Surface characterizations of color thresholds. *Journal of the Optical Society of America A, Optics and Image Science, 7,* 783–789. [PubMed]

Ruderman, D. L., & Bialek, W. (1994). Statistics of natural images: Scaling in the woods. *Physical Review Letters, 73,* 814–817. [PubMed]

Sankeralli, M. J., & Mullen, K. T. (2001). Bipolar or rectified chromatic detection mechanisms? *Visual Neuroscience, 18,* 127–135. [PubMed]

Schrödinger, E. (1920). Grundlinien einer Theorie der Farbenmetrik im Tagessehen. *Annalen der Physik, 4,* 397–426.

Stiles, W. S. (1946). A modified Helmholtz line element in brightness-colour space. *Proceedings of the Physical Society of London, 58,* 41–65.

tePas, S. F., & Koenderink, J. J. (2004). Visual discrimination of spectral distributions. *Perception, 33,* 1483–1497. [PubMed]

Tolhurst, D. J., Ripamonti, C., Párraga, C. A., Lovell, P. G., & Troscianko, T. (2005). A multiresolution color model for visual difference prediction. In *APGV '05: Proceedings of the 2nd Symposium on Applied Perception in Graphics and Visualization* (pp. 135–138). New York: ACM.

Tolhurst, D. J., Tadmor, Y., & Chao, T. (1992). Amplitude spectra of natural images. *Ophthalmic and Physiological Optics, 12,* 229–232. [PubMed]

Vos, J. J., & Walraven, P. L. (1972a). An analytical description of the line element in the zone-fluctuation model of colour vision—I. Basic concepts. *Vision Research, 12,* 1327–1344. [PubMed]

Vos, J. J., & Walraven, P. L. (1972b). An analytical description of the line element in the zone-fluctuation model of colour vision—II. The derivation of the line element. *Vision Research, 12,* 1345–1365. [PubMed]

Wachtler, T., Sejnowski, T. J., & Albright, T. D. (2003). Representation of color stimuli in awake macaque primary visual cortex. *Neuron, 37,* 681–691. [PubMed]

Wandell, B. A. (1982). Measurement of small color differences. *Psychological Review, 89,* 281–302. [PubMed]

Webster, M. A., & Mollon, J. D. (1991). Changes in colour appearance following post-receptoral adaptation. *Nature, 349,* 235–238. [PubMed]

Webster, M. A., & Mollon, J. D. (1994). The influence of contrast adaptation on color appearance. *Vision Research, 34,* 1993–2020. [PubMed]

Webster, M. A., & Mollon, J. D. (1997). Adaptation and the color statistics of natural images. *Vision Research, 37,* 3283–3298. [PubMed]

Wichmann, F. A., & Hill, N. J. (2001). The psychometric function: I. Fitting, sampling, and goodness of fit. *Perception & Psychophysics, 63,* 1293–1313. [PubMed] [Article]

Wyszecki, G., & Fielder, G. H. (1971). Color-difference matches. *Journal of the Optical Society of America, 61,* 1501–1513. [PubMed]

Wyszecki, G., & Stiles, W. S. (1982). *Color science concepts and methods, quantitative data and formulae*. New York: Wiley.

Xu, H., Yaguchi, H., & Shioiri, S. (2002). Correlation between visual colorimetric scales ranging from threshold to large color difference. *Color Research and Application, 27,* 349–359.

Zaidi, Q., & Halevy, D. (1993). Visual mechanisms that signal the direction of color changes. *Vision Research, 33,* 1037–1051. [PubMed]

Zaidi, Q., & Shapiro, A. G. (1993). Adaptive orthogonalization of opponent-color signals. *Biological Cybernetics, 69,* 415–428. [PubMed]

Zaidi, Q., Spehar, B., & DeBonet, J. (1998). Adaptation to textured chromatic fields. *Journal of the Optical Society of America A, Optics, Image Science, and Vision, 15,* 23–32. [PubMed]

Zhang, X. M., & Wandell, B. A. (1996). A spatial extension to CIELAB for digital color image reproduction. *Proceedings of the Society for Information Display, 96,* 731–734.

Zhang, X. M., & Wandell, B. A. (1998). Color image fidelity metrics evaluated using image distortion maps. *Signal Processing, 70,* 201–214.